RADIONUCLIDE CONCENTRATIONS AND RADIATION HAZARD ASSESSMENT IN THE SOIL OF OTJIWARONGO, NAMIBIA

A MINI-THESIS

SUBMITTED IN PARTIAL FULFILMENT

OF THE REQUIREMENTS FOR THE DEGREE OF

MASTER OF SCIENCE IN NUCLEAR SCIENCE

OF

THE UNVERSITY OF NAMIBIA

BY

NAEMAN TUYOLENI KAPOFI

200727745

September 2020

Supervisor: Professor James Oyedele

(Department of Physics, University of Namibia)

Co-Supervisor: Dr Gotfried Uiseb

(Department of Chemistry and Bio-Chemistry, University of Namibia)

Abstract

The natural radioactivity and associated hazards in soil samples collected from the town of Otjiwarongo, Namibia, have been studied by gamma ray spectroscopy. The town was divided into ten geographical areas and five soil samples were collected across each area. The samples were dried, homogenized and 500 g of each sample was placed in a clearly-labelled 500 mL polythene bottle and sealed for four weeks. HPGe detector was subsequently used to obtain gamma ray spectra of the samples. The intensities of selected gamma lines were used to determine the activity concentrations of the primordial radionuclides ^{238}U, ^{232}Th, and ^{40}K in the soil samples. The mean activity concentrations of the radionuclides in the ten geographical areas vary from 37.6 ± 7.4 to a high of 97.8 ± 46.2 Bq/kg for ^{238}U, from 81.9 ± 16.7 to a very high of 852.8 ± 533.0 Bq/kg for ^{232}Th and from 498.7 ± 55.7 to 807.1 ± 94.5 Bq/kg for ^{40}K. All these mean activity concentrations are higher than the corresponding world-wide average values of 33.0 Bq/kg, 45.0 Bq/ kg and 420.0 Bq/kg for ^{238}U, ^{232}Th and ^{40}K respectively, according to United Nations Scientific Committee on the Effects of Atomic Radiation (UNSCEAR) 2000 report. Furthermore, the mean activity concentrations of some of the radionuclides in some areas are more than double those of the other areas thus indicating that the distribution of radionuclides in the soil of the town is not uniform. In order to assess the hazards associated with the radionuclides, different radiation hazard parameters such as absorbed dose rate, effective dose rate, radium equivalent activity (Ra_{eq}), and external radiation hazard index (Hex), were calculated from the activity concentrations of the radionuclides.

The mean absorbed dose rates in the ten areas vary from 90.0 ± 13.7 to 593.9 ± 347.2 nGy h^{-1} and are all higher than the world average value of 60.0 nGy h^{-1}. However, the

corresponding mean effective dose rates vary from 0.11 ± 0.01 to 0.73 ± 0.43 mSv/y which are all below the maximum permissible limit of 1 mSv/y, according to the International Commission on Radiological Protection (ICRP) reference level for public exposure control. Furthermore, the mean effective dose rates in seven of the areas are relatively low and below 0.2 mSv/y while those in the other three areas are relatively high and above 0.2 mSv/y. These results indicate that the level of radiation varies across the town and it is low in seven geographical areas but higher in three areas. The mean values of the radium equivalent activity in the ten areas vary from 197.9 ± 31.5 to a very high value of 1379.5 ± 815.7 Bq/kg. Again, the mean Ra_{eq} in the seven geographical areas are low and below the maximum permissible limit of 370 Bq/kg while they are high and above the permissible limit in the other three areas. Similarly, the mean values of H_{ex} in the seven geographical areas are below the maximum permissible limit of unity but they are above the permissible limit in the other three areas. These results confirm that the level of ionizing radiation in most areas of Otjiwarongo is well-below the maximum permissible limit while the level in three other areas of the town is high and the hazard indices are above the maximum permissible limit.

Dedication

This thesis is dedicated to my mother “Miina Frans” and my late father “Paulus Kapofi Gepard,” as well as to all my lovely siblings.

Declarations

I Naeman Tuyoleni Kapofi, hereby declare that this study is my own and is a true reflection of my research work and that this work or any part thereof has not been submitted for a degree at any other institution of high learning. No part of this thesis may be reproduced, stored in any retrieval system, or transmitted in any form or by means (e.g. electronic, mechanical, photocopying, recording, or otherwise) without the prior permission of the author or the University of Namibia in that behalf.

I Naeman Tuyoleni Kapofi, grant the University of Namibia the right to reproduce this thesis in whole or in part, in any manner, which the University of Namibia may deem fit.

11/09/2020

Naeman Tuyoleni Kapofi **Date**

Acronyms

UNAM	University of Namibia
IAEA	International Atomic Energy Agency
MHSS	Ministry of Health and Social Services
HPGe	High Purity Germanium
ICRP	International Commission on Radiation Protection
NORM	Naturally Occurring Radioactive Material
UNSCEAR	United Nations Scientific Commission on Radiation Effects of Atomic Radiation
WNA	World Nuclear Association

Acknowledgements

Firstly, I would like to thank God for his protection and blessings during this study. Secondly, I wish to express my profound gratitude to my mentor and supervisor Professor, James Akindele Oyedele, for an excellent supervision and guidance during this project. I would like also to extend my sincere thanks to my co-supervisor, Dr Gotfried Uiseb, as well as to Mr Andrew Shimboyo, Mr Erastus Taapopi, Ms Monica Nambinga, and the Department of Physics of the University of Namibia, for their support and encouragement during this study. I am equally grateful to the Municipality of Otjiwarongo for the support provided during the collection of soil samples.

List of tables

List of figures

List of appendices

Contents

CHAPTER 1

1. Introduction

1.1. Radioactivity

Radioactivity is a process whereby radiation is released or given off by unstable atomic nuclei or radioisotopes [1]. The radiation given off or emitted by naturally occurring radioisotopes into the environment is known as background radiation. Unstable radionuclides in soils, rocks, water, and air are sources of natural background radiation [2]. If the background radiation is high, it could pose a health hazard as it may increase the risk of cancer. Consequently, the measurement of background radiation has been of interest to many scientists worldwide [3, 4]. The concentration of naturally occurring radionuclides can vary with location and altitude. This leads to variation in background radiation in any given environment. The widely distributed concentrations of radionuclides in nature depends on the local geological conditions and as a result vary from place to place [5]. About 70% of the natural background radiation comes from the earth crust including rocks and soils [6].

An unstable radioisotope may undergo decay series to reach a lighter stable nucleus or nuclei which may decay further either by alpha (α), beta (β) or gamma (γ) emission [7]. However, some unstable radioisotopes such as ^{137}Cs, ^{22}Na and ^{60}Co can be "man-made" (i.e. produced in the laboratory) [8]. Thus, there is a distinction between "natural radioactivity"- radioactivity of naturally occurring unstable isotopes and "artificial radioactivity"- radioactivity of the man-made unstable isotopes. There are unstable isotopes or radioactive elements in the soil, rocks, water, and air around us [9].

Naturally Occurring Radioactive Materials (NORMs) includes common radionuclides like Uranium- ^{238}U, Thorium-^{232}Th, and Potassium-^{40}K and their decay products, such as Radium and Radon. These are long- lived elements which have always been present in the earth's crust and atmosphere since the beginning of life. In other words, living and non-living organisms have been continuously exposed to radiation mainly from naturally occurring radionuclides and cosmic rays in the atmosphere. Generally, most radionuclides are stable; however, those that are naturally unstable parent nuclides have long half-lives compared to the decay products. Each radionuclide has a unique half-life [10]. By definition, the "half–life" of a particular radionuclide, is the time it takes for a radionuclide to lose 50% of its activity by decay. Furthermore, there are three natural radioactive decay series in nature. These are the Uranium series, the Thorium series and the Actinium series. These decay series have parent radionuclides of Uranium- ^{238}U, Thorium -^{232}Th and ^{235}U respectively.

Exposure of living organisms, including human beings, to ionising radiation could be hazardous, such that the exposure may cause both Deterministic effects, which is an immediate biological damage (absorbed doses above threshold), and Stochastic effects, which is a prolonged biological damage (no threshold). Therefore, according to the International Radiation Safety Standards it is recommended for a human being not to receive an exposure greater than effective dose of 1.0 mSv y^{-1}, for the members of the public, and not greater than 20.0 mSv y^{-1}, for the radiation workers [2].

1.2. Statement of the problem

Namibia has many mineral resources like Uranium-238, and so the radioactivity in the soils of some areas and towns could be high. A number of studies have been carried out to determine the concentration of radionuclides or natural radioactivity in the soils of some towns in Namibia [11]. These important studies were supported by the University of Namibia (UNAM) and by different Ministries of the Republic of Namibia, and the nuclear equipment used in the studies were provided by the International Atomic Energy Agency (IAEA). However, the concentrations of radionuclides in the soils of the towns in the central part of the country have not been studied extensively. These towns include Otjiwarongo amongst others. Therefore, there is a need to determine the concentrations of radionuclides in the soil of Otjiwarongo and to assess the radiation level in the town in order to establish baseline data of radionuclide activity concentrations which will be useful for safety assessment and planning purposes in the town or in future studies.

1.3. Objectives of the study

The objectives of this study are to:

a) Determine the concentrations of the primordial radionuclides ^{40}K, ^{232}Th, and ^{238}U in the soil of Otjiwarongo and investigate the correlations between the concentrations.
b) Determine effective dose rates, different radiation hazard indices and to ascertain whether or not the concentrations of radionuclides in the soil of Otjiwarongo are of any radiological importance.
c) Provide baseline data of activity concentrations of radionuclides in the soils.

1.4. Significance and relevance of the study

The town of Otjiwarongo has a population of more than 21 000 and is situated about 240 km north of Windhoek. The town is an important service centre for the surrounding commercial farms and is a convenient base for day trips to the Waterberg Plateau Park and the well-known dinosaur footprints on the farm Otjihaenamaparero. The opening of the B2Gold Namibia mine and a Cement Plant near the town should boost the economy of the town and increase the population of the town. More importantly, the town is known for tourism and it is the main gate-way between the south and north of Namibia. The envisaged study will provide information on the background radiation level to which visitors and inhabitants of Otjiwarongo are exposed. It will also contribute to the baseline data of activity concentrations in the soils of Namibia.

CHAPTER 2

2. Literature review

2.1. Interaction of radiation with matter

The literature on radioactivity have indicated that radioactivity was discovered when radiation interacted with matter. Ionizing radiations which interact with matter may be alpha rays, beta rays, neutron rays, x-rays, or gamma rays, depending on the type of the radiation and energy of moving particle causing ionizing effects (removal of an electron from an atom of a matter). However, the degree of interaction of radiation or particle with matter depends on the rest mass and charges of the moving particle. For instance, particles like alpha and beta are charged, while gamma rays are not charged. Hence these three particles can have different ranges of interaction with matter. In terms of range of radiation, “Alpha radiation” has small range, whereas “Beta particle/radiation” has an intermediate range, while “Gamma radiation” has a high range which could cause transitional or permanent physical and chemical changes in the molecules that interact with the radiation [12]. The commonly known processes of ionizing radiation interaction with matter are Compton scattering, Photoelectric effect, and Pair production, as discussed in sub-section 2.1.1.

2.1.1. Processes of ionizing radiation interactions with matter

There are three main processes of ionizing radiation interaction with matter:

A. <u>Compton scattering</u>

This interaction occurs when an incident photon (an elementary particle) interacts with a loosely bound outer orbital electron of an atom of a particular matter. As this interaction is occurring, the photon loses part of its energy and a recoil electron is

released from atom's outer orbital of the atom. At the same time, the scattered photon is deflected through an angle (θ) which is proportional to the amount of energy lost. It has been demonstrated that the maximum energy loss occurs when the angle θ is 180˚ or when the photon is back scattered, whereas for small angle θ, less energy is lost. This type of radiation interaction is demonstrated in Figure 2.1.

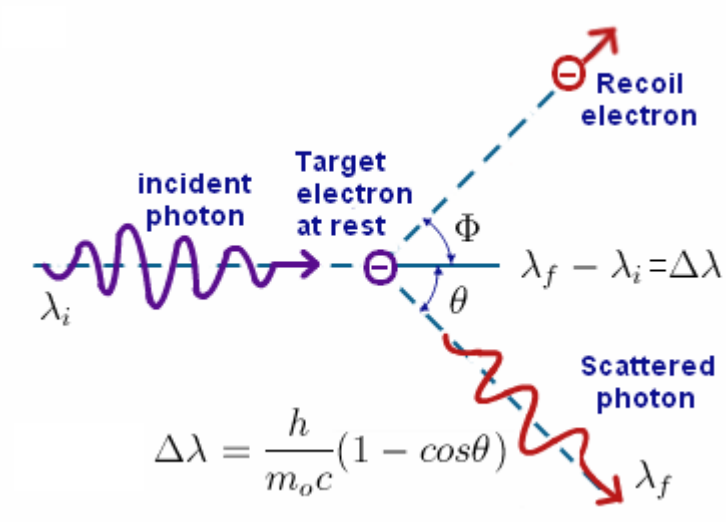

Figure 2.1: Compton effect *[13]*.

Compton equation:

$$\lambda_f - \lambda_i = \frac{h}{m_\circ c(1-\cos\theta)} \qquad (2.1)$$

where,

λ_f is the wavelength of incident rays after scattering,

λ_i is initial wavelength of the incident ray,

h is the Planck's constant,

$m_\circ$ is electron mass,

c is speed of light,

θ is the scattering angle of incident ray

$\lambda_f - \lambda_i$ is known as Compton shift.

B. Photoelectric effect

The photoelectric effect involves the interaction of low-energy incident photons with matter. During this interaction, an atom of the matter absorbs an incident photon of energy hν and an electron of particular energy is ejected. One example of photoelectric effect is when light rays with sufficient frequency strike a solid surface, resulting in emission of electrons from the matter, as shown in Figure 2.2. This effect may not take place if the incident ray does not have high frequency.

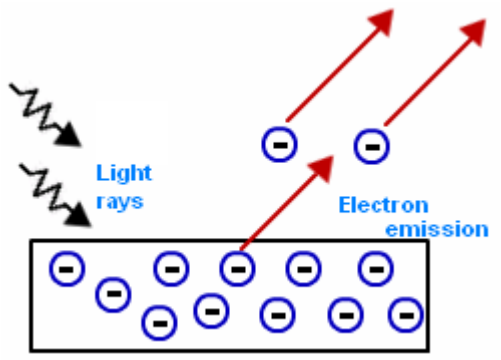

Figure 2.2: Photoelectric effect *[14]*.

The photoelectric effect is given by the equation:

$$\mathrm{KE}_{max} = h\nu - \Phi \qquad (2.2)$$

where,

$$E = h\nu \qquad (2.3)$$

KE is the kinetic energy of the emitted electron, $h\nu$ is the energy of the photon, while Φ is the work function and it is given as, $h\nu_{\circ}$.

A photon is a quantum of light energy or electromagnetic energy, and the threshold frequency of the incident light is the minimum frequency which can eject photo-electrons from a metallic surface. Equally, the threshold wavelength of the incident light is the maximum wavelength at which the incident light can eject photo-electrons from a metallic surface. The ejected electron is normally from the K- or L- shell of the atom while absorption edges occur at lower energies for the L, M, N electron shells of the atom [15].

Below are some characteristics of photoelectric effect

1) The photoelectric current increases with increase of the intensity of incident light, but it is independent of the frequency of incident light.
2) The maximum kinetic energy of an emitted electron increases with increase of the frequency and is independent of the incident light.
3) The process of photoelectric effect is instantaneous.

C. Pair production

The pair production effect is the generation of elementary particle and its anti-particle like electron and positron. This interaction will normally occur when a particular photon of certain energy interact with an atomic nucleus of a material as illustrated in Figure 2.3. This is one of the principal ways, in which high-energy gamma rays are absorbed in matter. However, for pair production to take place, the electromagnetic energy (photon), must be at least equivalent to the mass of two electrons. This means, mass "m" of a single electron is equivalent to 0.51 MeV of energy E as from Albert Einstein equation 2.4, in order to produce two electrons, the incident photon energy must be at least twice the energy of one electron. That is $2(mc^2)$ MeV, and photon energy in excess of this, will be converted into motion of the produced pair [5].

$$E = mc^2 \quad (2.4)$$

where, c is a constant equal to the speed of light.

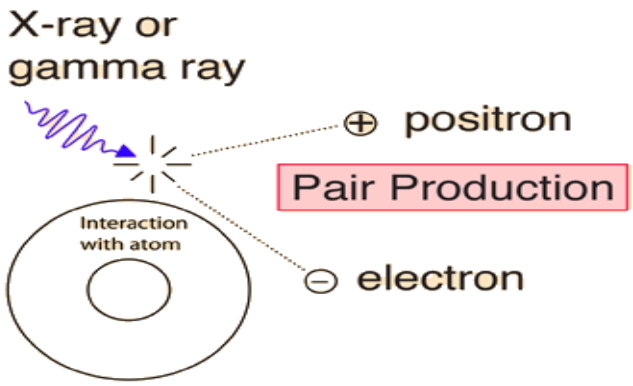

Figure 2.3: Pair production process *[16]*

Another process related to pair production is annihilation, which is a reaction in which particle and its antiparticle collide and disappear releasing energy. The most common annihilation on Earth occurs between an electron and its antiparticle, a positron. In other words, annihilation is the inverse of pair production as shown in Figure 2.4.

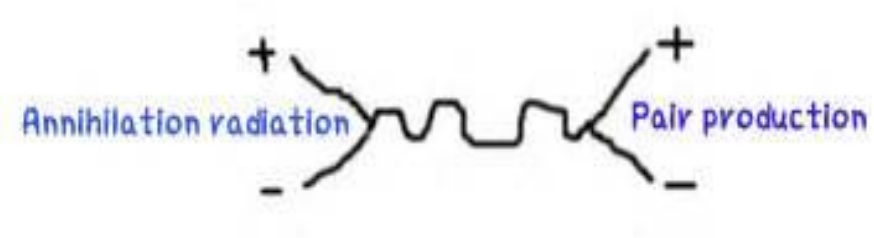

Figure 2.4: Annihilation and Pair production processes

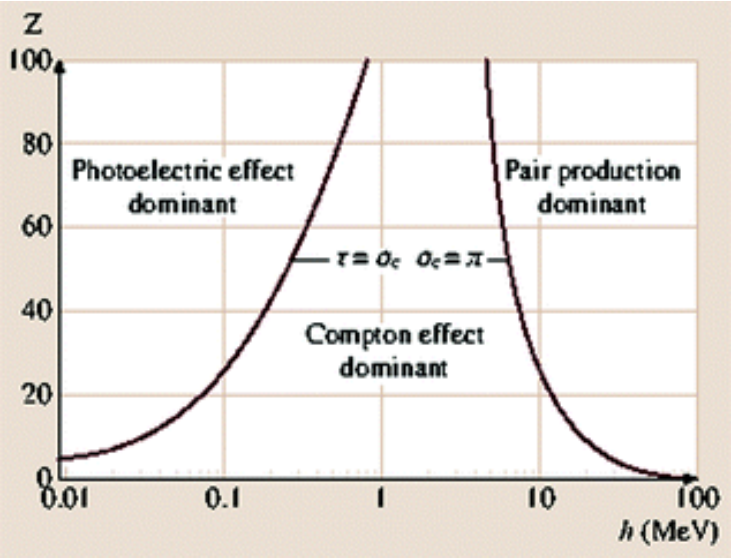

Figure 2.5: Types of radiation interactions with matter

The three processes of radiation interaction with matter could be described further graphically as shown in Figure 2.5. These processes depend on photon energy and on atomic number of the absorber (matter), Z. For instance, the photoelectric process is the predominant mode at relatively low energies and enhanced for materials of high atomic number, Z, while Compton effect is dominant at gamma-ray energies of roughly 0.1-10 MeV, in an absorber of relatively low Z value. The Pair production effect is dominant at high energy photon but also enhanced for absorber of higher Z value.

2.2. Radiation detection and measurement

There are different types of detectors for detecting ionization radiations, [15]. However, in order to detect emitted radiation, a correct detector must be used. Practically, a detector detects emitted radiation once it entered the detector and interact with the detector's atoms. Upon interaction with the detector's atoms some electrons

will be released from atoms of the detector, collected, and moulded into a voltage or current pulse for analysis by the electronic components of the detector system [17]. Some radiation detectors are discussed below:

2.2.1. HPGe detector

In this study, High-purity Germanium (HPGe) detector will be used to analyse soil samples. The HPGe detector is a semiconductor detector with p-i-n structure in which intrinsic region is sensitive to ionizing radiation, including gamma-ray and X-rays [17]. Liquid Nitrogen (LN2) is the most common coolant used in cooling HPGe detectors (-196.15 ^{o}C), in order to reduce the thermal generation of charge carriers. Additionally cooling is necessary because germanium has a relative low band gap, and leakage current induced noise destroys the energy resolution of the detector [15].

When photons interact with the material within the depleted volume of a detector, charge carriers like electrons are produced. Subsequently, these charge carriers are swept by the electric field to the collecting electrodes, where a preamplifier component coverts these charges into voltage pulses proportional to the energy deposited in the detector [17], as shown in Figure 2.6.

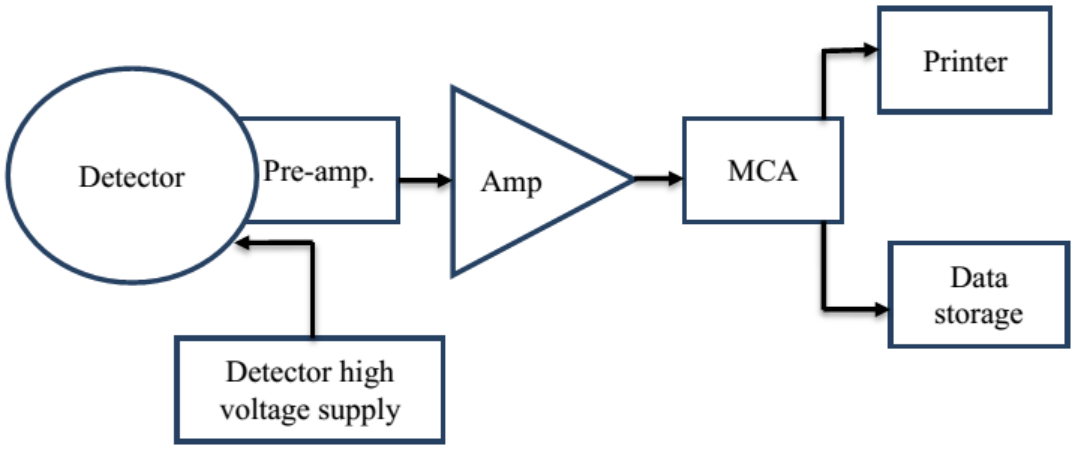

Figure 2.6: A diagram of gamma spectroscopic system *[17]*.

.

2.2.2. Geiger Muller counter (GM-tube)

A Geiger-Muller counter is also sometimes called a GM-tube. The GM-tube has a long tube (>30 cm) which is usually filled mainly with Argon gas and it operates under applied voltage. The tube is fitted with a metal cylinder (the cathode) and a thin conductive wire (the anode) mounted along the tube as illustrated in Figure 2.7.

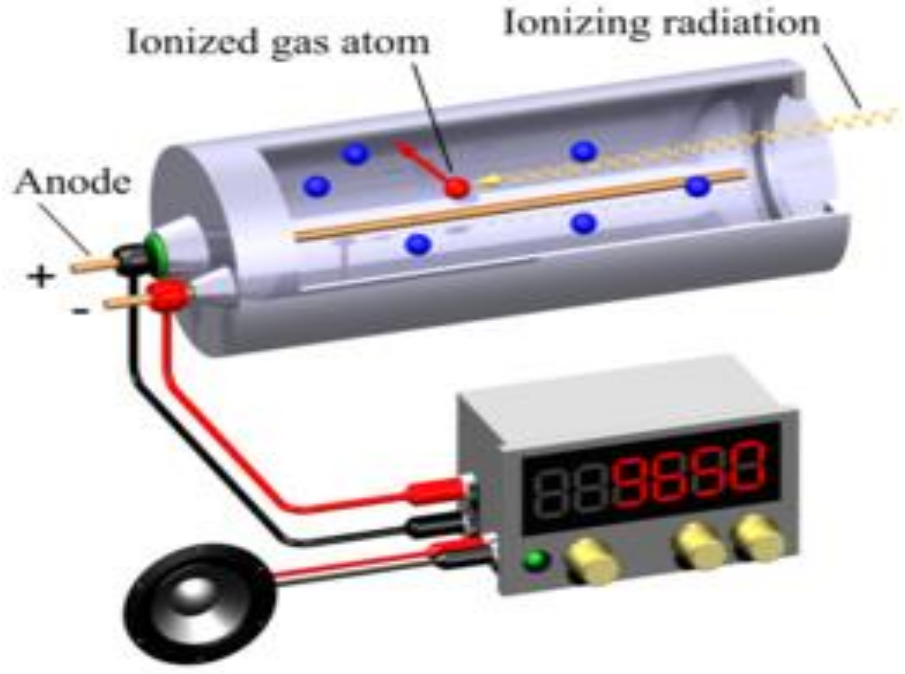

Figure 2.7: A typical diagram of GM-tube *[18]*.

The counter has a strong electric field between the cathode and anode electrode. The strong electric field created by the voltage across the tube's electrodes accelerates the positive ions towards the cathode and the electrons towards the anode. This leads to the build-up of ions in the tube causing amplification of signals, resulting into development of voltage pulse at anode output of the counter.

2.2.3. Scintillation counter

Scintillation counter involves the use of luminescent material (Scintillator). However, a good scintillator should be able to convert efficiently the energy deposited by a charged particle into detectable light. Radiation causes excitation of the atoms of scintillator and the atoms then return to the ground state by emitting photon (light) which is the quantitative information of the radiation. The emitted light is transferred into a photomultiplier tube. A fraction of these emitted photons/light is then converted into photoelectrons and then accelerated through an electric field toward electrode called "dynode." As dynode is stricken by each electron more secondary electrons are produced. This increases the number of electrons, leading to a significant number of electrons accelerated through the electrical field, resulting in the production of signal proportional to the light output of scintillation, which is proportional to the energy deposited by the emitted radiation.

2.2.4. Cloud chamber and Bubble chamber

The Cloud and Bubble Chambers are earlier devices developed over years that can show the presence of particles and reveal their properties by the tracks that they leave. However, due to higher advancement of research technologies, these devices have been superseded. The two devices work on a common principle of a charged particle that passes through a cloud chamber, and leaves a path of detectable ionised particles, as discussed below:

Cloud chamber – As shown in Figure 2.8, the principle of the cloud chamber involves an ionising radiation passing through the cold damp air in the chamber and it leaves track of droplets which is a characteristic of the ionising radiation. For instance, an alpha particle passing through the cloud chamber would leave a thicker and short track

of droplets than that of a beta particle because the alpha particle is more ionising and larger (loses its energy more rapidly).

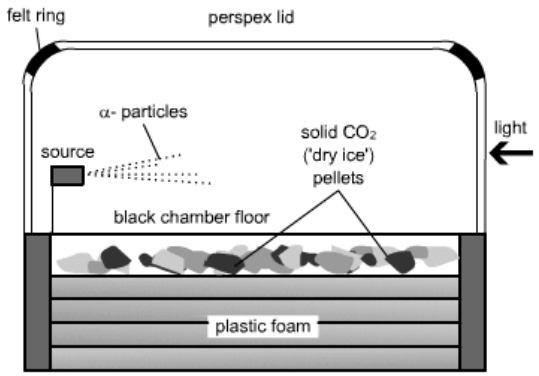

Figure 2.8: A typical diagram of a Cloud chamber system *[19]*.

Bubble chamber – The chamber consists of a tank of superheated liquid hydrogen kept just on the verge of boiling. As a particle moves through the liquid, it ionizes the hydrogen and leaves tiny bubbles in the chamber. For the charged particles to follow curved paths, the tank is kept under strong magnetic fields as shown in Figure 2.9.

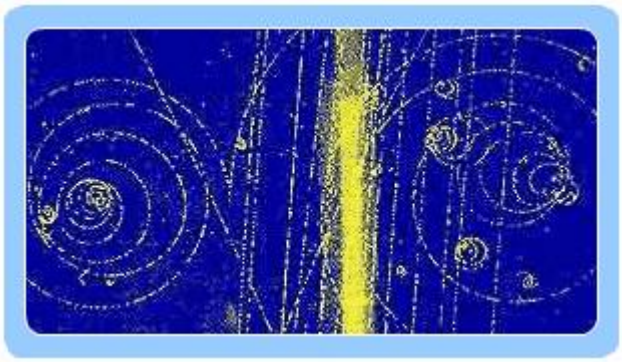

Figure 2.9: A diagram of a Bubble chamber in strong magnetic fields *[20]*.

2.3. External Exposure

There have been many surveys conducted to determine radioactivity levels in soils, which can in turn be related to the absorbed dose rates in air [2]. However, the level of radioactivity and external exposure (outdoors) depend on geology of the given area. For instance, higher radioactivity level associates with igneous rocks, such as granite, and some shales and phosphate rocks have also a relatively high level of radioactivity [21], while lower radioactivity level associates with sedimentary rocks. External exposures outdoor arise from terrestrial radionuclides present at trace levels in all soils [22]. That is, the external exposure mostly attributed to background radiation, which contributed by terrestrial elements such as ^{238}U, ^{232}Th, and ^{40}K.

Moreover, some source radionuclides like Uranium and Thorium may be in equilibrium with their daughter radionuclides in their respective decay series. However, the decay may lead to dissociation of the decayed radionuclides from the source radionuclide into environmental transfer mechanisms. This however could cause relocation of radionuclides from one point to the other, leading to high chance of other possible exposure types such as internal exposure caused by ingestion of radionuclides via eating food and drinking water.

2.4. Review of studies on NORMs in soil

In any given environment, the level of Naturally Occurring Radioactive Material (NORM) varies with the geology of the area, and it tends to be influenced by man-made activities. Therefore, there is a need to reflect on similar previous studies done nationally and internationally, and compare the results with those that will be obtained in this study. According to the recent World Nuclear Association (WNA) report, the

average dose received by all human from background radiation is around 2.4 mSv/y, which varies depending on the geology and altitude where people live, ranging between 1 and 10 mSv/y, but can be more than 50 mSv/y [23].

Nationally, there have been a number of studies on the natural radioactivity in the soils of Namibia, especially in the Western part of the country where many uranium mines are situated [11]. Some of these towns are Walvis Bay, Swakopmund, Usakos and Wlotzkasbaken. The mean activity concentrations of the radionuclides in the four towns vary from a low of 18.6 ± 4.6 Bq/kg to a high of 69.6 ± 26.3 Bq/kg for ^{238}U, from a low of 23.8 ± 8.4 to a high of 91.1 ± 41.0 Bq/kg for ^{232}Th and from 460.3 ± 76.2 to a high of 959.5 ± 194.7 Bq/kg for ^{40}K. The resulting mean annual effective dose of the three towns is 0.11 mSv/y, which is much below the maximum permissible limit of 1.0 mSv/y [11].

A related local study on radioactivity of the four major towns in northern Namibia was also recently conducted [24], in order to provide baseline data on the radiation level in the northern region. The average concentrations of radionuclides in these towns vary from a low of 7.5 ± 2.3 to a high of 14.2 ± 3.3 Bq/kg for ^{238}U; from a low of 5.8 ± 2.6 to a high of 24.9 ± 6.1 Bq/kg for ^{232}Th and from a low of 52.1 ± 28.7 to high of 380.1 ± 112.9 Bq/kg for ^{40}K. These concentrations were used to calculate the mean absorbed dose rate and the mean annual effective dose. The obtained mean effective dose of 21 ± 16 µSv, shows that the region has a normal background radiation [24].

Internationally, in Iran, Europe and India elevated annual effective doses from background radiation were recorded, with people exposed to an annual dose of more than 100 mSv up to 260 mSv dose. To be specific, at Ramsar in Iran, some 200, 000 people are exposed to more than 10 mSv/y [23]. Moreover, the highest level of

background radiation affecting a substantial population is recorded in Kerala and Madras States in India where some 140,000 people receive doses which averaged over 15 mSv/y from gamma radiation, which was similar to doses from radon gas [23]. Similarly, elevated levels occur in Brazil and Sudan, with average exposures up to about 40 mSv/y to many people, with the highest level of natural background radiation recorded on a Brazilian beach of 800 mSv/y, but people do not live there [23].

2.5. Hazards associated with NORMs

The effects of ionizing radiation in humans can occur immediately after an exposure to radiation (Deterministic effects) or later in life long after the exposure (Stochastic effects). Both effects involve successive processes of biological damage at both molecular, cellular, tissue and whole organism levels. The deterministic effects occurs when absorbed dose threshold is exceeded (not common with NORMs) and this can cause serious damage to organ and tissue. The stochastic effects has no threshold level, and this damage consists primarily of damage to the nuclear material in the cell, causing radiation-induced cancer to develop in a proportion of exposed persons or hereditary disease in their offspring [2].

The exposure to ionizing radiation depends on the magnitude of the dose absorbed, the exposure time, type of organ or tissue exposed. The inhalation of short-lived decay products of ^{222}Rn, and the decay products of ^{220}Rn, and their successive deposition along the walls of the various airways of the bronchial tree provide the main pathway for radiation exposure of the lungs [21]. The exposure is predominantly produced by the alpha, beta and gamma radiation emitted by different radionuclides.

CHAPTER 3

3. Materials and Methods

3.1. Study area

Otjiwarongo is a town in the Otjozondupa region of Namibia and it is situated approximately 245 km, north of the capital city, Windhoek, as shown in Figure 3.1. The town of Otjiwarongo was divided into ten (10) geographical areas for the purpose of sample collection as shown in Figure 3.2.

Figure 3.1: Map of Namibia showing the location of Otjiwarongo town

3.2. Sample collection

Five (5) samples were collected from each of the ten geographical areas as show in Figure 3.2. This gives a total number of 50 soil samples collected from the town. All the sites chosen were away from roads, buildings, railway lines, industrial or agricultural sites and rivers. Soil samples were collected from undisturbed areas at a depth of about 2cm - 5cm below the soil surface as shown in Figure 3.3. Personal Protective Equipment (PPE) used during soil collection include gloves and dust masks. Each sample collected was about 1kg, and was placed in a plastic bag which was labelled according to the geographical area of collection. After the sampling exercise, all samples were then transported to the Nuclear Physics Laboratory in the Department of Physics of the University of Namibia (UNAM), Windhoek, for preparation and analysis. A photograph of the collection of soil sample at a site is shown in Figure 3.3. Also, a photograph of the team that collected soil samples in Otjiwarongo is shown in Figure 3.4.

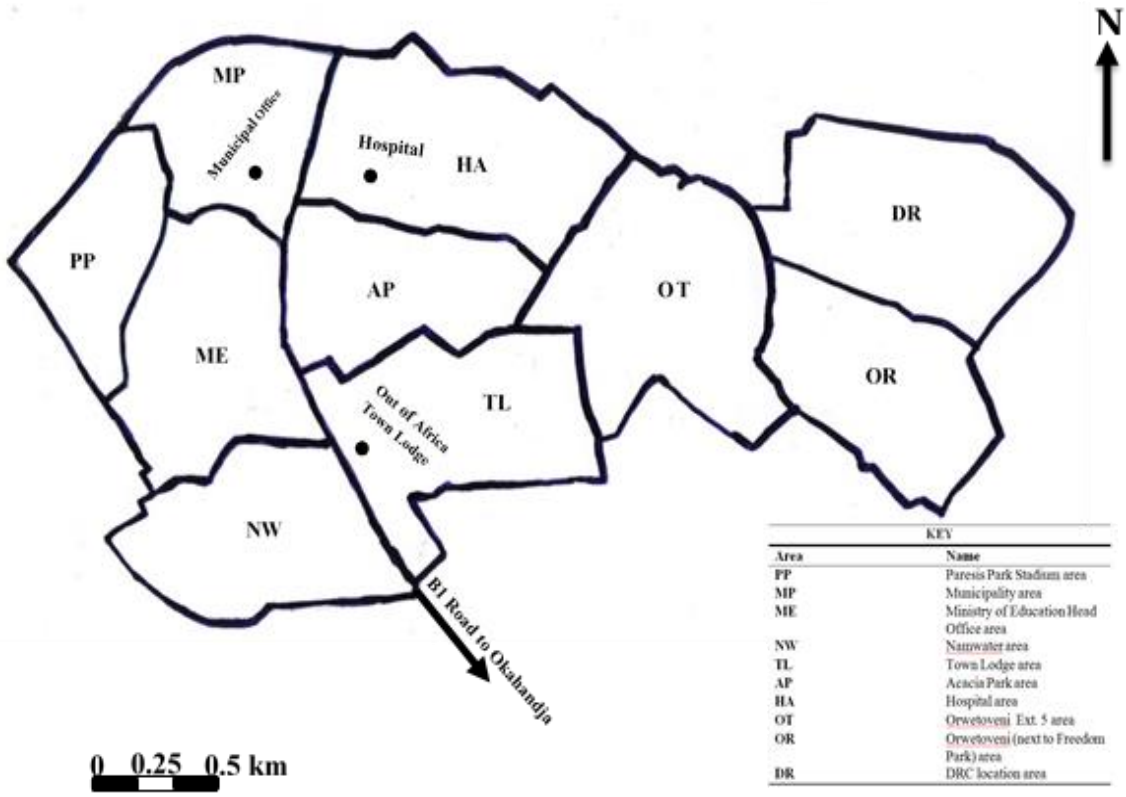

Figure 3.2: A map showing the geographical areas where soil samples were collected in Otjiwarongo

Figure 3.3: Collection of soil samples in Otjiwarongo

Figure 3.4: A photograph of the team from UNAM that collected soil samples in Otjiwarongo. From left is Mr E. Taapopi, Mr N. Kapofi (the researcher), Ms L. Hanga, Prof J. Oyedele and Mr S. Shimboyo

3.3. Sample preparation

As soon as the soil samples were delivered at the Nuclear Physics Laboratory at UNAM, each sample's plastic bag was opened to allow the soil sample to dry at room temperature for a period of about 72 hours as shown in Figure 3.5. After this drying period, stones, vegetation and organic matters were removed from each sample and the dried soil sample was sieved through a 2 mm mesh screen such as the one shown in Figure 3.6. After all the samples were sieved, 500 g of each sample was carefully weighed and placed in a 500 ml polythene bottle such as the one shown in Figure 3.7. All the bottles were then tightly closed and stored at room temperature (as shown in Figure 3.8) for about four weeks to ensure radioactive equilibrium, between ^{226}Ra, ^{232}Th and their progeny before the samples were analysed using the HPGe detector.

Figure 3.5: Drying of soil samples

Figure 3.6: The Sieve used in sample preparation

Figure 3.7: A 500 ml polythene bottle used for the soil samples

Figure 3.8: Soil samples stored in the laboratory for radioactive equilibrium prior to radio-analysis

3.4. Detector used

As indicated under sub-section 2.2.1, the HPGe detector was used in this study to analyse the soil samples. The HPGe p-type detector has a relative efficiency of 20% (Canberra model GC2519), with a high resolution of 1.0 keV FWHM at 122 keV and 1.9 keV FWHM at 1332 keV. As shown in Figure 3.9, the detector is inside a Canberra Model 737 lead shield, with a thickness of 10 cm.

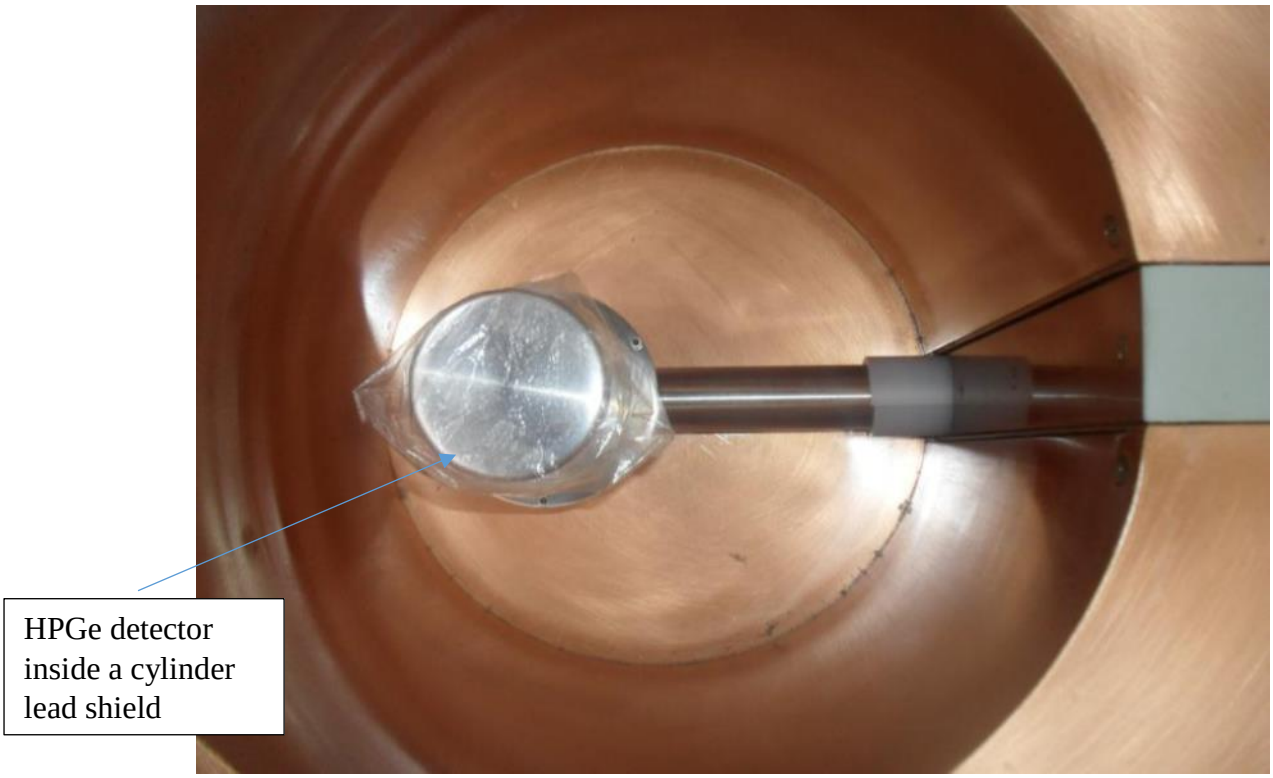

Figure 3.9: HPGe detector inside a Canberra Model 737 lead shield

The Canberra Model 737 lead shield has also a graded 1.5 mm copper and 1.0 mm tin lining with an outer jacket of 9.5 mm thick low carbon steel. The liquid nitrogen was supplied from a Model 7915-30 Cyrostat (Base Model 7915-30) to the detector for cooling purposes, as shown in Figure 3.10.

Figure 3.10: A Model 7915-30 Cryostat for supplying LN2 to the HPGe detector inside a Canberra Model 737 lead shield

Other components of the detector system include a Model 2100 Bin/Power Supply providing mounting space for a Model 1786 LN2 monitor and a High Voltage Power Supply (HVPS) Model 9645. It also includes a Model 9660 Digital Signal Processor (housing a Model 2016 Amplifier-TCA, an Analog to Digital Converter (ADC)), an Acquisition Interface Module (AIM 556A) Multichannel Analyser (MCA) as shown in Figure 3.11. The software that was used in analysing the acquired spectral was "Genie® 2000" (version 2.0).

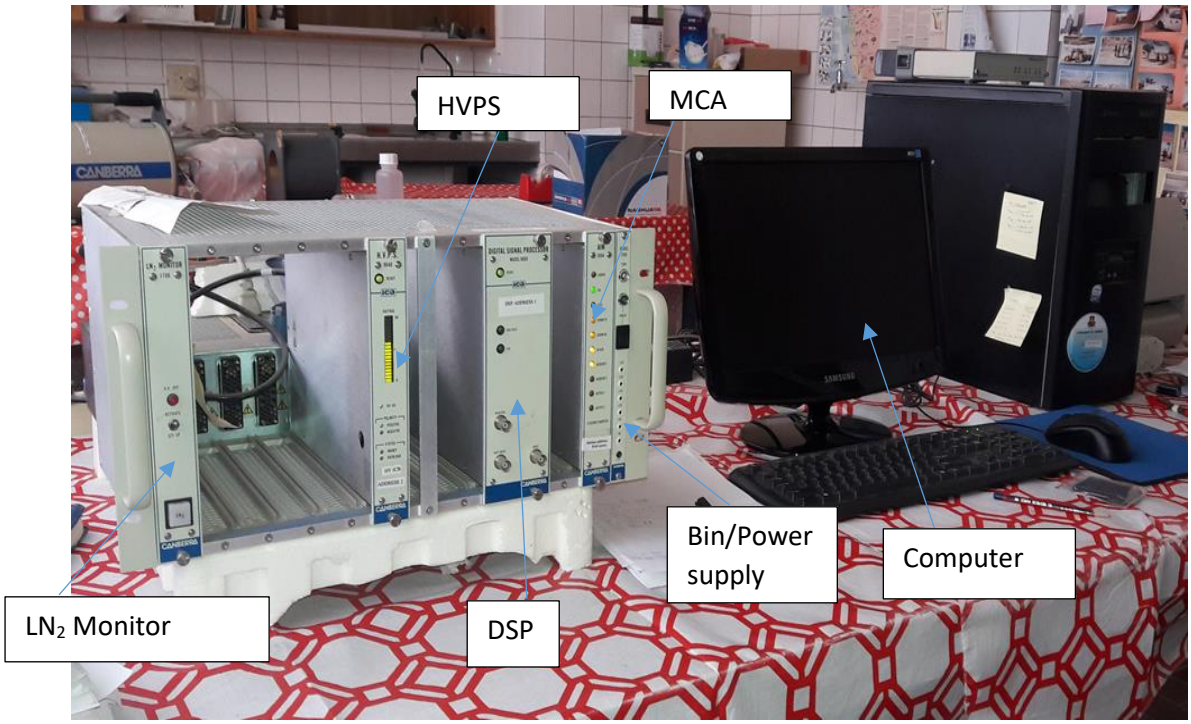

Figure 3.11: Components of the detector system

The operation of the HPGe system used in this study is similar to what has been discussed under sub-section 2.2.1. The system has electric field (produced by high voltage) between electrodes and photon interaction within this region produces charge carriers which are swept by the electric field to their collecting electrodes, where a charge sensitive preamplifier converts this charge into a voltage pulse proportional to the energy deposited in the detector [17]. Once the voltage pulse is produced, it travels to the amplifier that shapes and amplifies the signal. The signal then move to a digital signal processor (DSP) that quantifies the energy from the detector and sends it to a multi-channel analyser (MCA). The MCA can scan a whole energy range and records the number of pulses they count depending on their pulse height (which is proportional to the incident gamma photon energy) the pulses are divided into channels according to their energies and the memory accumulator consists of 4096 individual channels.

Automatically the system produces a histogram of data accumulated in the MCA memory which represents a plot of the number of counts (intensity) versus channel number (γ-photon energy) for all pulses acquired in a specified time interval.

Generally, the HPGe detector is highly sensitive to many factors like background radiation, sample matrix, sample geometry, counting time detector resolution and detector efficiency. Due to this level of sensitivity, the system has to be cooled, in order to reduce thermal noise, and to freeze moisture that could be in the system. The coolant used in this study was Liquid Nitrogen (LN2).

3.5. Calibration of detector and measurement on reference materials

As part of analytical procedures, the HPGe detector was calibrated prior to the analysis of the soil samples. The calibration was achieved using three point sources, ^{22}Na, ^{60}Co and ^{137}Cs. Energy calibration involves identifying the gamma rays within a measured spectrum by matching the energies of the gamma rays with those emitted by known radionuclides. In this study, the three known point sources (radionuclides) were used for calibration of the detector to provide a well-defined energies within the energy range of interest, where a relationship between the peak position in the spectrum and the corresponding gamma-ray energy is obtained. The analysis of the gamma-emitting sources with known specific energy values was performed prior to sample analysis in order to identify the peak energies in the spectra. Each peak energy was then assigned to its corresponding channel, thereby establishing efficiency level of the detector as shown in Table 3.1.

Table 3.1: Point sources used for energy-channel calibration of the detector system

Radionuclide	Energy (keV)	Channel number
^{137}Cs	661.75	1118.29
^{60}Co	1173.41	1982.83
^{22}Na	1274.75	2154.07
^{60}Co	1332.67	2251.94

The three point sources were selected to cover a wide energy range over which the spectrometer is to be used. The spectrum of the point sources was measured (known energies) and compared the measured peak position with energies (Figure 3.12). The Genie 2000 software calibration function was used to obtain a linear fit of the calibration as shown in Figure 3.13. Moreover, some reference materials were further used in the calibration of the detector system. These reference materials are RGU-1, RGTh-1 and RGK-1. The spectra of the reference materials are shown from Figure 3.14 to Figure 3.16, and the photograph of the reference materials is shown in Figure 3.17. That is, the obtained spectra of the reference materials could be used to identify and quantify radionuclides present in the soil samples.

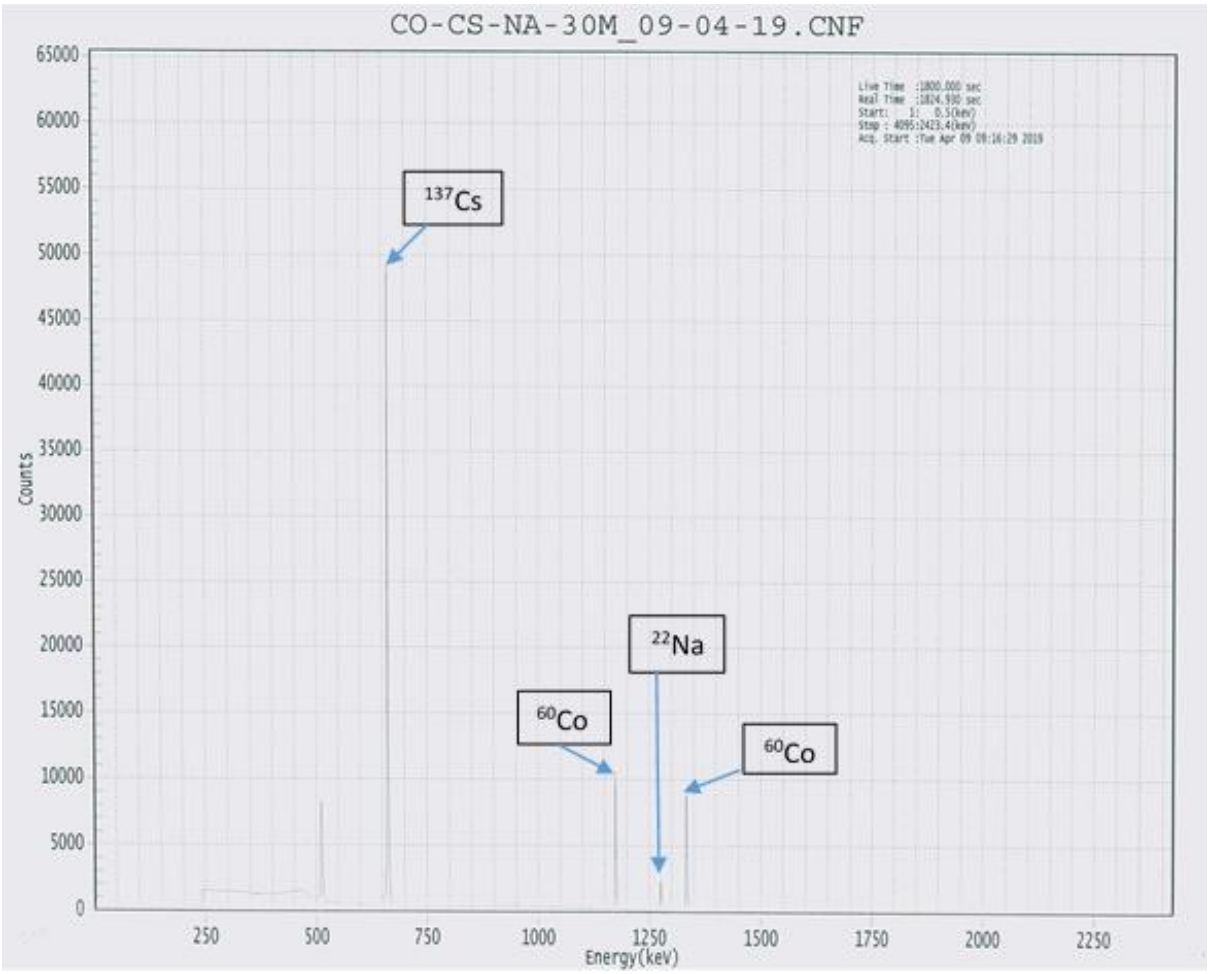

Figure 3.12: Calibration spectra

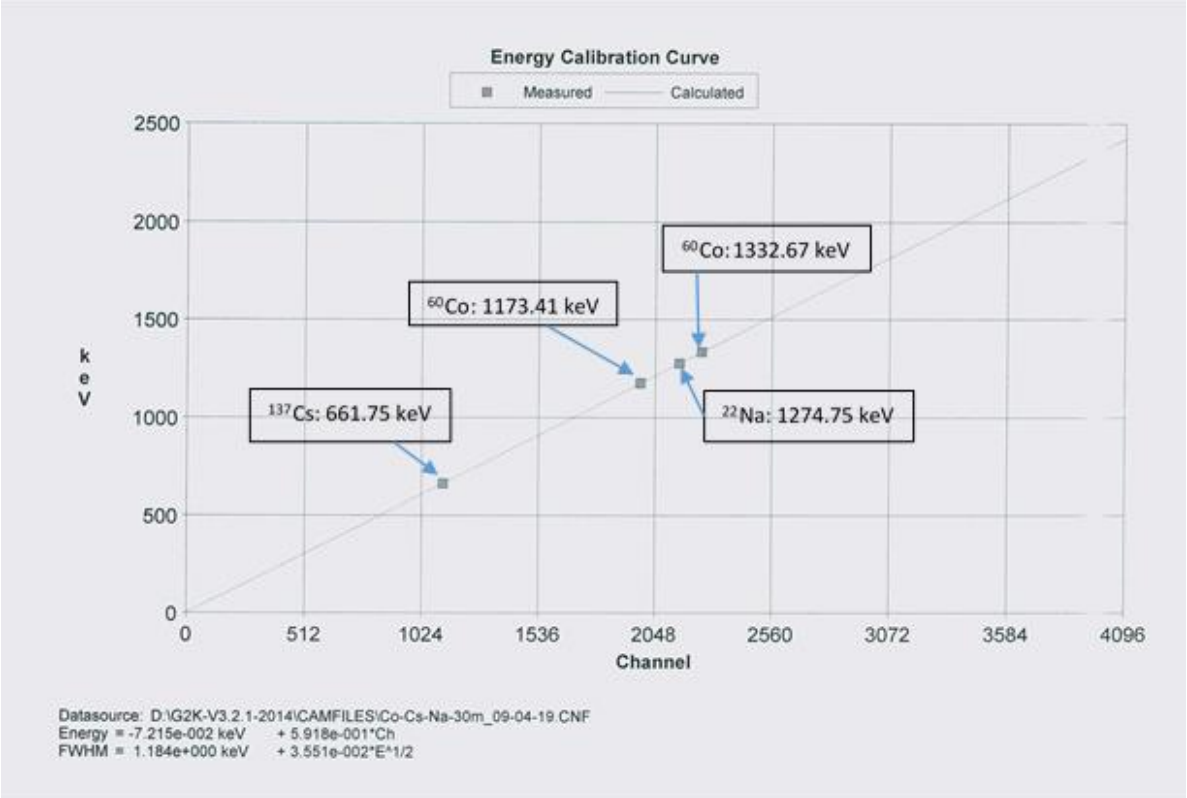

Figure 3.13: Calibration curve

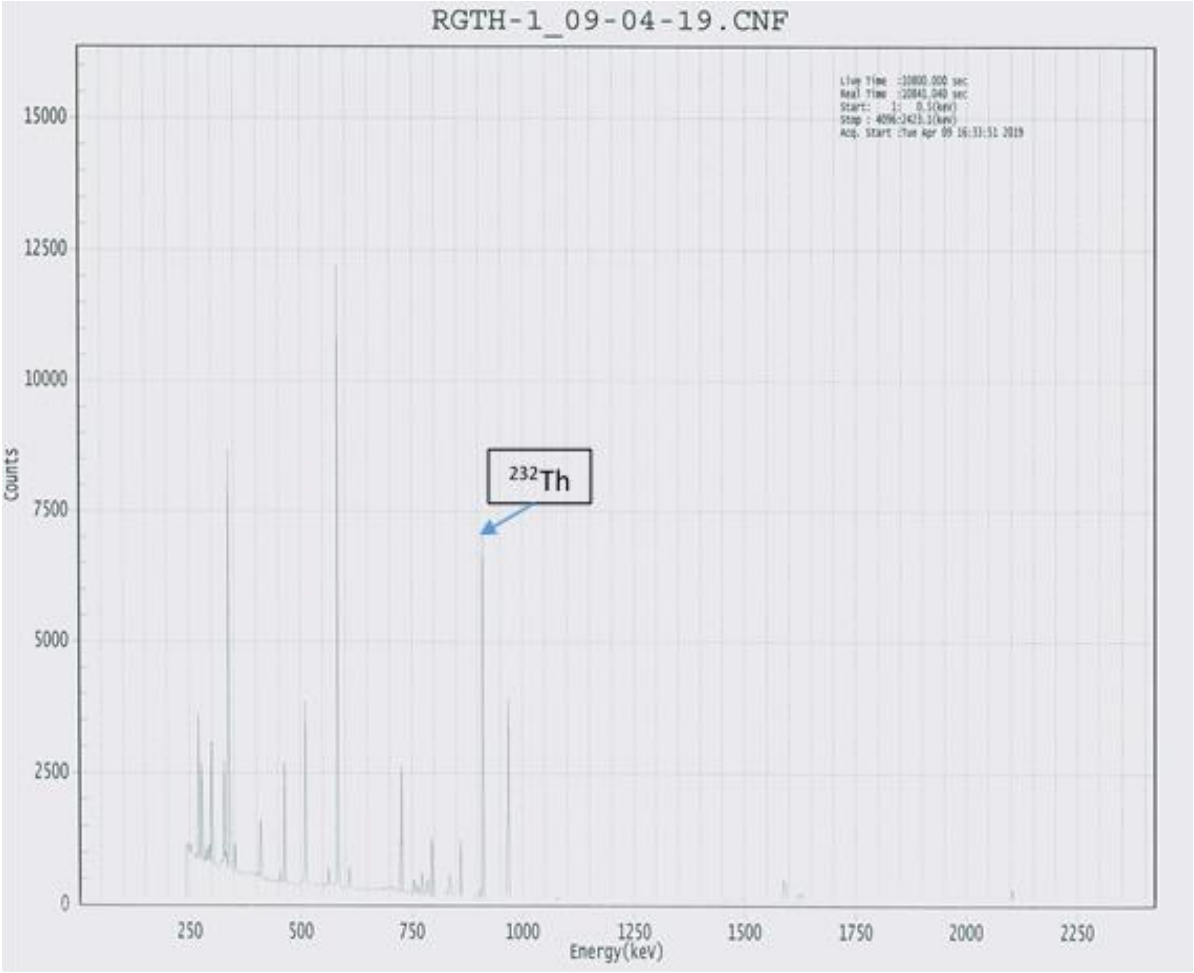

Figure 3.14: The spectra of ^{232}Th reference material (RGTH-1)

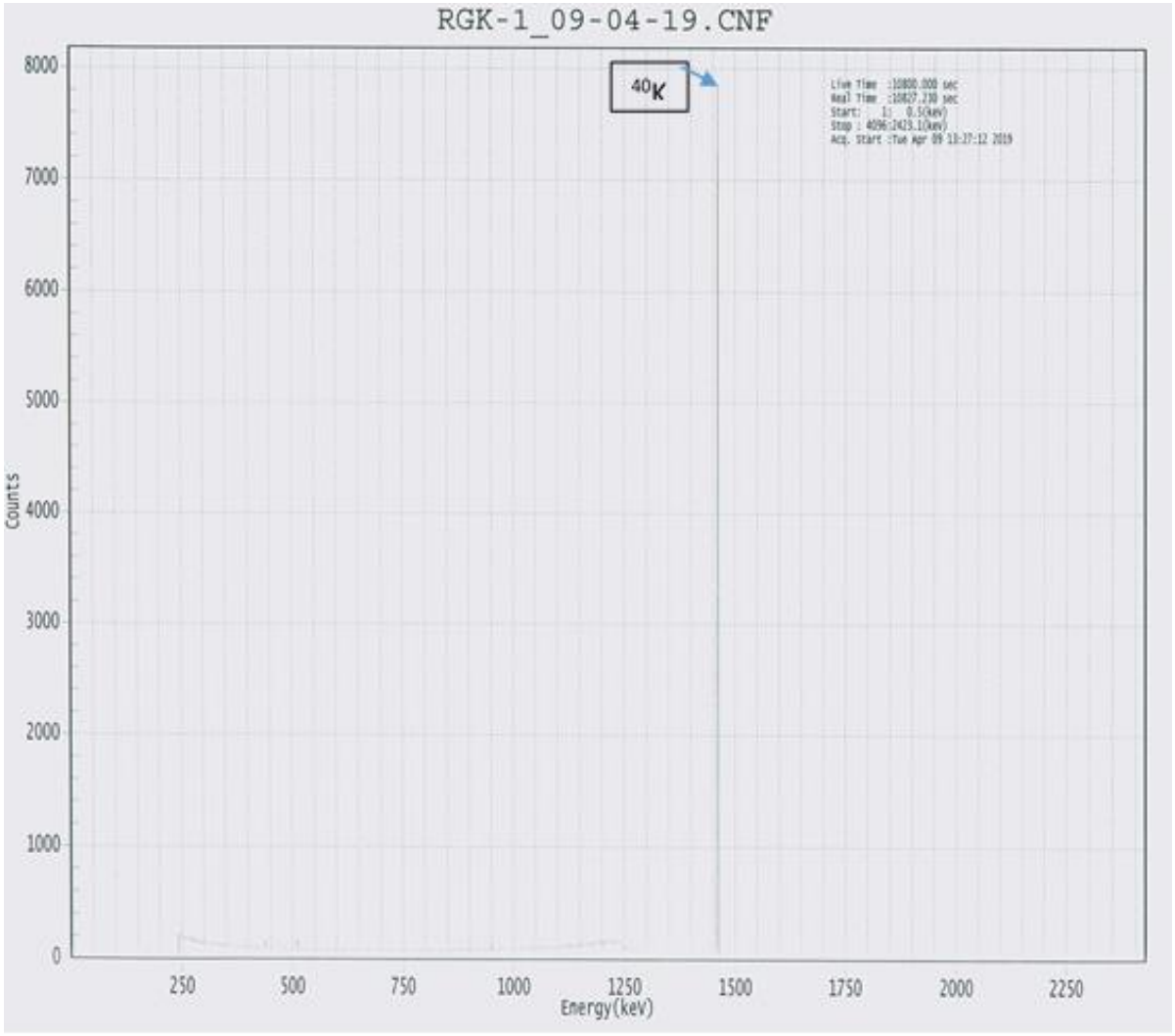

Figure 3.15: The spectra of ^{40}K reference material (RGK-1)

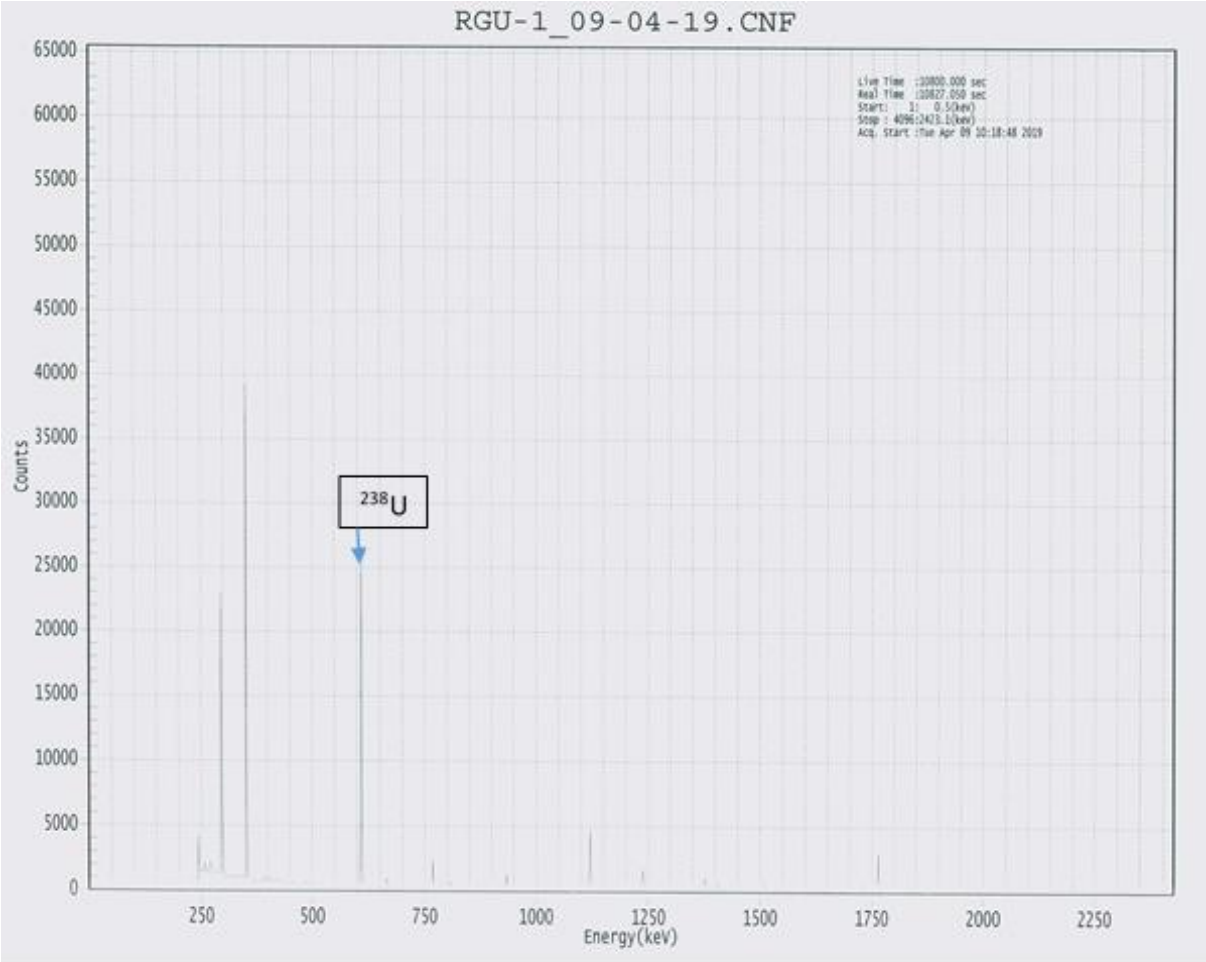

Figure 3.16: The spectra of ^{238}U reference material (RGU-1)

Figure 3.17: A photograph of the IAEA reference materials

3.6. Background Counting

Upon completion of the calibration, the background radiation around the detector was counted for 3 hours. The results show a very low background radiation – no peak energy of interest was observed as could be seen in Figure 3.14. The background radiation was also counted for 12 hours with an empty polythene bottle of the same dimensions as the soil sample bottles (similar bottles) placed on-top of the detector (inside the lead-shield). Again, the background radiation was very low.

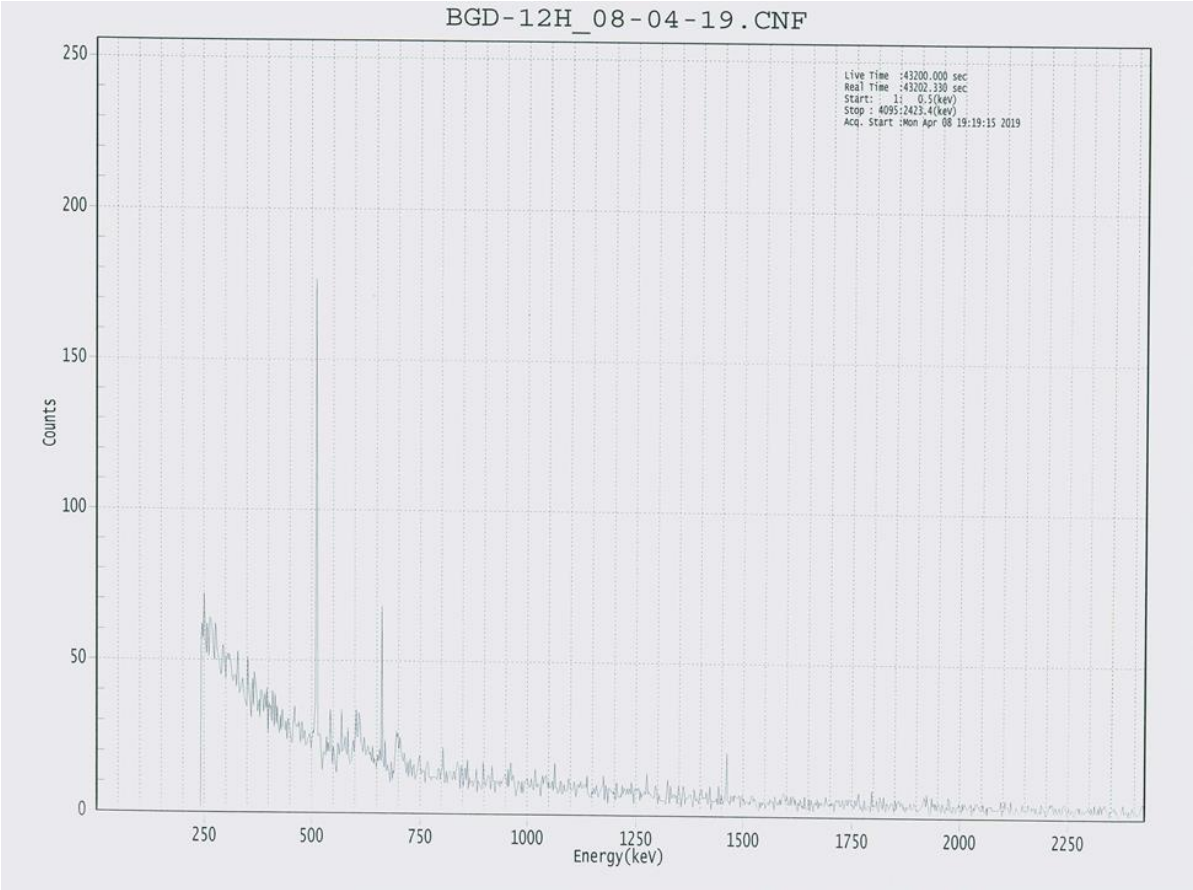

Figure 3.18: Background spectrum

3.7. Measurement on soil samples

Following the calibration and background radiation measurement (section 3.5 and 3.6 respectively), each reference material was placed on the detector (inside the lead shield) and counted each for a period of 10800 seconds (3 hours). Similarly, each soil sample was also placed on the detector and counted for 3 hours as shown in Figure 3.15.

Figure 3.19: Counting of the radiation emitted by a soil sample

All soil samples had the same dimensions, and they were placed on the detector to ensure same geometry of counting (same position), and each counted for the same period of 10800 seconds. As indicated earlier, the activity concentrations of interest in the soil samples are that of ^{238}U, ^{232}Th and ^{40}K radionuclides, and the contents of them in the samples were determined by the measurements of the photo peaks of gamma rays from ^{214}Bi (609.318keV), ^{228}Ac (911.07 keV), and ^{40}K (1460.70 keV) respectively.

3.8. Determination of activity concentrations

Gamma spectroscopy was used for the analysis of all soil samples. Each measurement produced peaks of different heights in the energy spectrum. The area "A" under a photo peak depends on the concentration of the radionuclide in a sample [25].

The activity concentration of each of the three radionuclides was evaluated from specific energy intensity. The activity concentration of ^{238}U was determined from the intensity of 609.31 keV gamma transition line of ^{214}Bi, while the activity concentration of ^{232}Th was determined from 911.07 keV gamma line of ^{228}Ac, and the activity concentration of ^{40}K is directly taken from its characteristic of 1460.70 keV gamma ray energy peak.

The same operating condition of the detector system was kept constant throughout the measurement. Since *net area* "A" under a photo peak depends on the concentration "C" of the radionuclide in a sample as stated above; then

$$\boldsymbol{A \propto C} \quad \text{or} \quad \boldsymbol{A = KC} \tag{3.1}$$

$$\text{that is, } \boldsymbol{K = A/C} \tag{3.2}$$

K is a constant of proportionality, for a given element or radionuclide.

The constant of proportionality K^x_{strd} for a given element in the standard was calculated using the general expression 3.3.

$$K^x_{strd} = \frac{A^x_{strd}}{C^x_{strd}} \tag{3.3}$$

where A^x_{strd} and C^x_{strd} are the respective net peak area and the activity concentration of a specific radionuclide in the standard. It is expected that each K value of a specific

radionuclide (x) in its corresponding standard (K^x_{strd}) is equal to its value in each sample (K^x_{sample}). Hence, from equation (3.3), K^x_{strd} was used to calculate the activity concentration of each radionuclide (x) in each sample using the general expression 3.4.

$$C^x_{sample} = \frac{A^x_{sample}}{K^x_{strd}} \quad (3.4)$$

where, A^x_{sample} is the net area under a peak of a specific radionuclide (x) in a sample, which is measured from a spectrum.

Moreover, the mean activity concentration of each radionuclide in each area was used to calculate other radiological parameters like absorbed dose rate, annual effective dose, and hazard indices.

3.9. Absorbed dose and annual effective dose

Absorbed dose (D):

Absorbed dose is a measure of the energy absorbed per unit mass, given in a unit of Gray (Gy). The activity concentrations of the radionuclides ^{40}K, ^{232}Th, and ^{238}U indicate the amount or quantity of these three radionuclides in the soil but not the amount of energy absorbed in unit mass. Hence, in this study the mean activity concentrations of these three radionuclides in each area were used to calculate the corresponding absorbed dose rate using the following equation:

$$\boldsymbol{D = 0.462A_u + 0.604A_{Th} + 0.0417A_k} \quad (3.5)$$

where D is the dose rate (nGy h^{-1}) at 1m above the ground due to ^{238}U, ^{232}Th and ^{40}K in the soil, while A_u, A_{Th} and A_k are the activity concentrations of ^{238}U, ^{232}Th and ^{40}K in Bq/kg, respectively. The constants 0.462, 0.604, 0.0417 are the conversion factors (nGy h^{-1}) for ^{238}U, ^{232}Th and ^{40}K respectively [2]. The mean absorbed dose rate in each geographical area was calculated.

Annual effective dose (B):

The effective dose is a quantity that takes into account the biological damage caused by different radiation [2]. To estimate the annual effective dose from absorbed dose rate, two factors are of importance: the conversion coefficient from Gy h^{-1} to Sv h^{-1} and the occupancy factor [17]. The conversion factor of 0.7 Sv Gy^{-1} is used to convert absorbed dose rate in air to human effective dose. The outdoor occupancy factor of 0.2 assumes that an average individual stays outdoors for about 4.8 hours a day [2]. Therefore, the absorbed dose rate of each area was used to calculate the corresponding annual effective dose (mSv y^{-1}), using the following relation:

$$\boldsymbol{B(nGy\,h^{-1}) = D \times 0.008760 \times 0.7 \times 0.2\,mSv\,y^{-1}} \qquad (3.6)$$

where D is any value of the absorbed dose rate.

3.10. Hazard indices

The hazard indices which are normally used to indicate the level of exposure are also calculated. One of these indices is the radium equivalent activity (Ra_{eq}) given by the following equation:

$$\boldsymbol{Ra_{eq} = A_{Ra} + 1.43\,A_{Th} + 0.077\,A_k} \qquad (3.7)$$

where A_{Ra} , A_{Th}, and A_k are respectively activity concentrations of ^{238}U, ^{232}Th and ^{40}K in Bq/kg and it is assumed that there is secular equilibrium between ^{238}U and ^{226}Ra (same activity concentration). The other hazard indexes are reflecting external exposure (H_{ex}) and internal exposure (H_{in}) respectively and are they are given by;

$$\boldsymbol{H_{ex} = {A_{Ra}}/{370} + {A_{Th}}/{259} + {A_k}/{4810}} \quad (3.8)$$

$$\boldsymbol{H_{in} = {A_{Ra}}/{185} + {A_{Th}}/{259} + {A_k}/{4810}} \quad (3.9)$$

where, A_{Ra}, A_{Th}, and A_k are as defined earlier and it is assumed that there is secular equilibrium between ^{238}U and ^{226}Ra.

CHAPTER 4

4. Results and discussions

The activity concentrations of the nuclides ^{238}U, ^{232}Th, and ^{40}K measured in the soil samples collected across the town of Otjiwarongo are presented and discussed in this chapter. The radiological hazards associated with the activity concentrations are also discussed in this chapter.

4.1. Activity concentrations

The mean activity concentrations of the primordial radionuclides ^{238}U, ^{232}Th, and ^{40}K in the soil samples collected from the ten geographical areas of the town of Otjiwarongo are presented in Table 4.1 and shown in Figure 4.1. The range of activity concentration of the radionuclide in each area is also shown in the same Table. Furthermore, the concentration of each radionuclide measured in each of the 50 soil samples are shown in Appendix I.

Table 4.1: Mean activity concentrations of ^{238}U, ^{232}Th and ^{40}K in different geographical areas of Otjiwarongo. The range of values are given in parenthesis

Area	Mean activity concentration (Bq/kg)		
	^{238}U	^{232}Th	^{40}K
PP	**46.9** ± **10.1** (36.8 - 60.4)	**99.9** ± **29.2** (70.5 - 135.6)	**543.1** ± **49.1** (478.6 - 596.9)
MP	**37.6** ± **7.4** (25.4 - 44.2)	**88.0** ± **43.4** (38.6 - 144.7)	**498.7** ± **55.7** (411.2 - 556.1)
ME	**42.0** ± **8.5** (30.8 - 54.2)	**98.1** ± **27.3** (68.9 - 135.7)	**510.3** ± **43.8** (457.7 - 571.4)
NW	**37.8** ± **3.2** (32.2 -40.0)	**89.0** ± **26.9** (71.9 - 136.3)	**562.2** ± **40.4** (520.4 - 627.6)
TL	**40.3** ± **6.6** (29.9-45.0)	**96.5** ± **25.6** (58.3 - 119.7)	**573.5** ± **25.7** (551.0 - 602.0)
AP	**47.0** ± **9.2** (36.0 - 58.2)	**146.1** ± **55.7** (97.4 -227.5)	**554.1** ± **35.5** (515.3 - 596.9)
HA	**41.0** ± **6.7** (33.7 - 49.1)	**81.9** ± **16.7** (61.2 - 103.8)	**517.4** ± **13.6** (501.0 - 535.7)
OT	**46.0** ± **15.8** (27.2 - 64.5)	**222.0** ± **107.2** (88.6 - 334.4)	**698.0** ± **52.2** (642.9 - 760.2)
OR	**97.8** ± **46.2** (32.3 - 153.5)	**852.8** ± **533.0** (200.0 -1397.0)	**807.1** ± **94.5** (693.9 - 882.7)
DR	**56.4** ± **11.6** (45.8 - 72.9)	**275.1** ± **113.5** (163.4 - 429.0)	**794.6** ± **77.7** (709.2 - 898.0)
Mean	**49.3** ± **23.1**	**204.9** ± **278.2**	**604.3** ± **119.5**

As could be observed in Table 4.1 and Figure 4.1, the mean activity concentration of ^{238}U varies from a low value of 37.6 ± 7.4 Bq/kg at MP area to a high value of 97.8 ± 46.2 Bq/kg at OR area. The mean activity of ^{232}Th varies from a low value of 81.9 ±

16.7 Bq/kg at HA area to a high value of 852.8 ± 533.0 Bq/kg at OR area. Also the mean activity of ^{40}K varies from a low value of 498.7 ± 55.7 Bq/kg at MP area to a high value of 807.1 ± 94.5 Bq/kg at OR area. This shows that the mean radioactivity concentrations of ^{232}Th and ^{40}K are relatively high across the ten geographical areas and they are much higher than the corresponding world-wide mean values of 45 Bq/kg and 420 Bq/kg, respectively. More especially, the mean activity concentration of ^{232}Th at OR area is extremely high and very much higher than its world-wide mean value. However, the mean radioactivity concentrations of ^{238}U in most of the areas (Table 4.1, column 2 and Figure 4.1) are only slightly higher than the world-wide mean value of 33 Bq/kg [2]. The highest mean activity concentrations of all three radionuclides (^{238}U, ^{232}Th and ^{40} K) are in the OR area, while the least mean activity concentrations of ^{40}K and ^{238}U are both in the MP area.

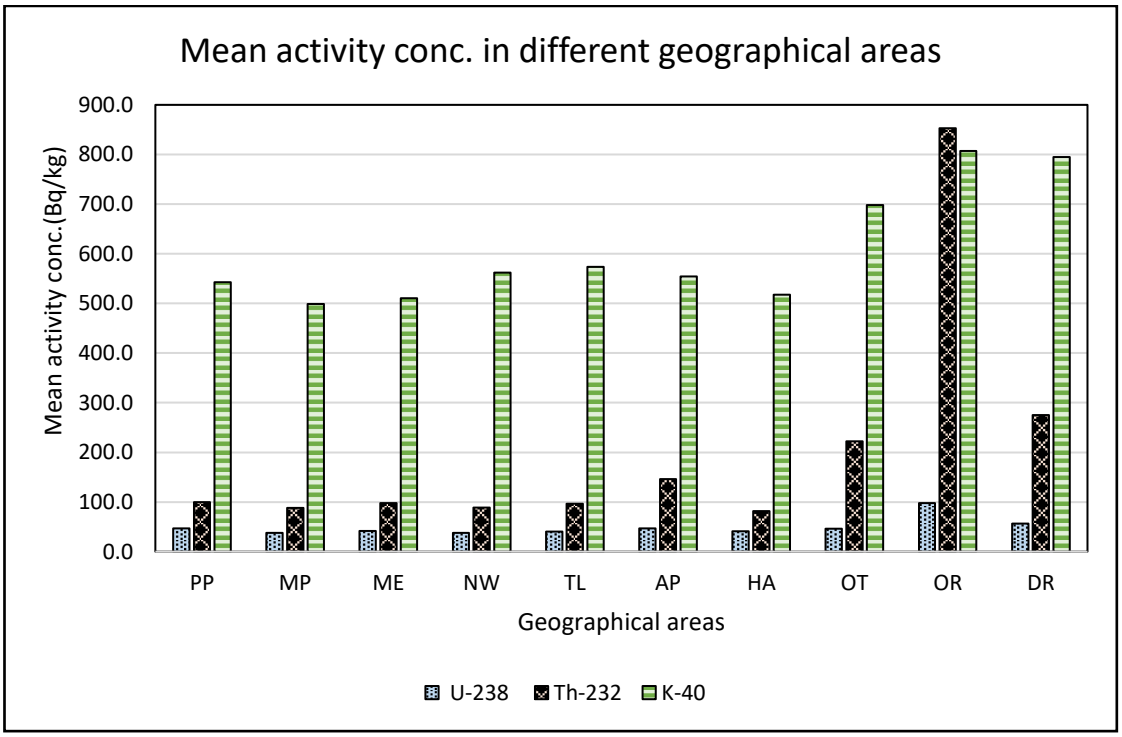

Figure 4.1: The mean activity concentrations of ^{238}U, ^{232}Th, and ^{40}K in the ten geographical areas

In fact, the mean activity concentrations of some of the radionuclides (e.g.^{232}Th) in some areas (e.g. OR) are more than double those of the other areas (e.g. MP) thus indicating that the distribution of radionuclides in the soil of the town is not uniform. The high activity concentrations of ^{232}Th in the samples could be due to the geology of the area, while the relatively high activity concentration level of ^{40}K in the samples could be due to the fact that there is no agricultural or mining activities in the town which could affect ^{40}K activity concentration level in the soil. Therefore, a relatively high activity concentrations of ^{40}K across the town could be attributed to its natural abundance in the soil.

4.2. Statistical analysis of the activity concentrations of radionuclides in the soil samples collected across Otjiwarongo

The statistical analysis of the activity concentrations of all collected soil samples is presented in Table 4.2. This includes skewness which describes the statistical distribution curve whether it is to the left (negative) or right (positive), and Kurtosis which is a measure of outliers in the distribution [26].

Table 4.2: Statistics of the results obtained in the measurement of activity concentrations in Otjiwarongo

Descriptive statistics	Activity concentration (Bq/kg)		
	^{238}U	^{232}Th	^{40}K
Mean	49.3	204.9	604.3
Standard Dev.	23.1	278.2	119.5
Median	43.8	115.3	563.8
Skewness	2.9	3.3	1.1
Kurtosis	9.5	10.8	0.3
Minimum	25.4	38.6	411.2
Maximum	153.5	1397.0	882.7
Range	128.1	1358.0	471.4

As indicated in Figure 4.2(a) and Table 4.2, the activity concentrations of ^{238}U have a skewness of 2.9 and kurtosis of 9.5. These values show a positive Skewness of ^{238}U activity concentration distributions around the mean value of 49.3 Bq/kg in most of the samples, and with a relatively high kurtosis.

Similarly, the statistical analysis of ^{232}Th activity concentrations has a skewness of 3.3 and a kurtosis of 10.8, with only a few of the activity concentrations around the mean value of 204.9 Bq/kg, while a high kurtosis shows that the activity concentrations are widely spread (with outliers).

The activity concentrations of ^{40}K show a Skewness of 1.1 and a Kurtosis of 0.3, which are representative of an asymmetric activity distribution, with most of the

samples' activities around the mean value of 604.3 Bq/kg, and no outliers, as shown in Figure 4.4.

The frequency distributions of activity concentrations of ^{238}U, ^{232}Th and ^{40}K, in the fifty soil samples collected from Otjiwarongo are shown in Figure 4.2, 4.3 and 4.4 respectively.

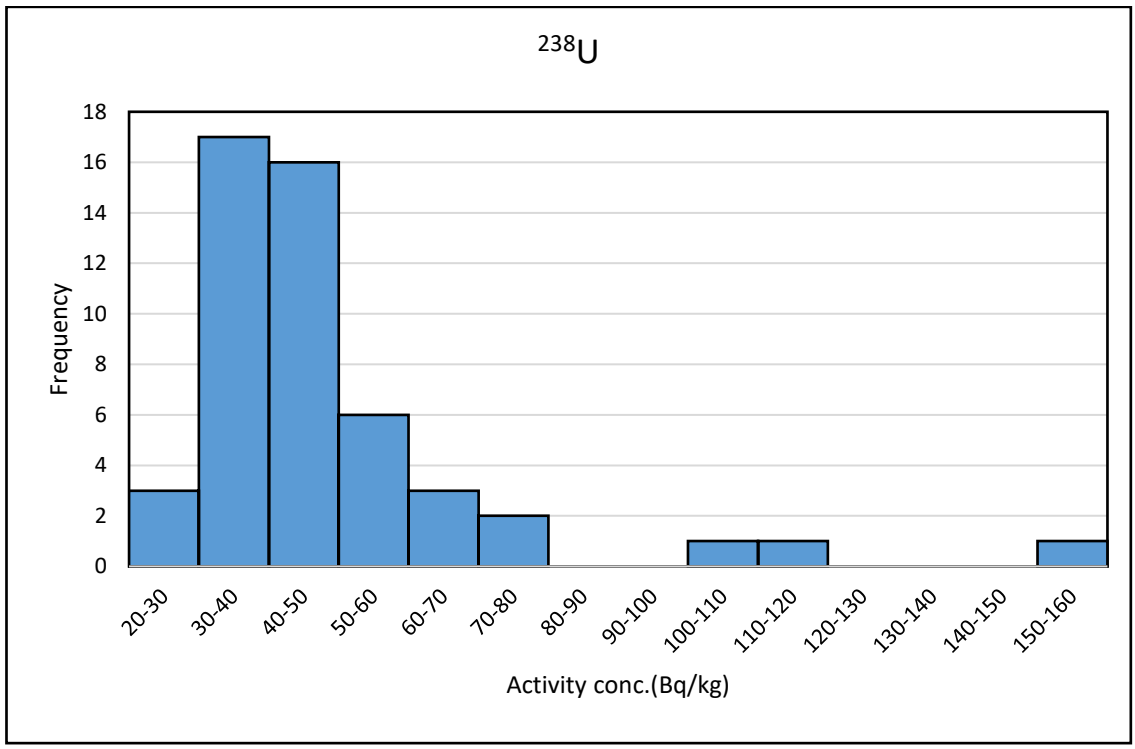

Figure 4.2: Frequency distributions of activity concentrations of ^{238}U in the soil samples

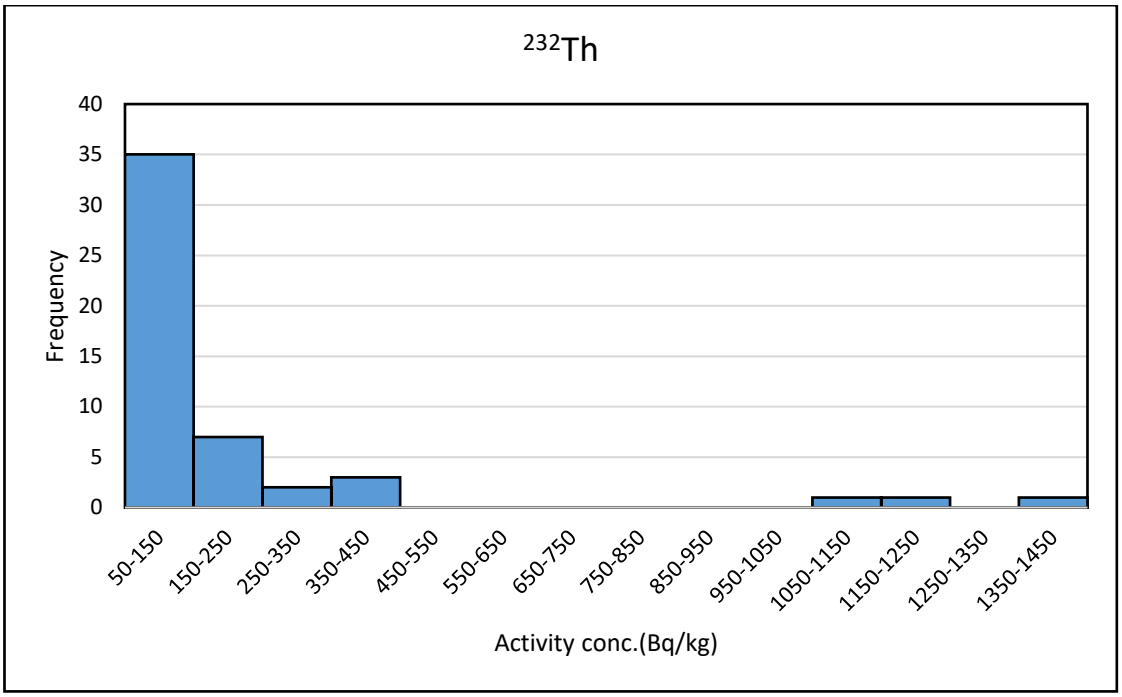

Figure 4.3: Frequency distributions of activity concentrations of ^{232}Th in the soil samples

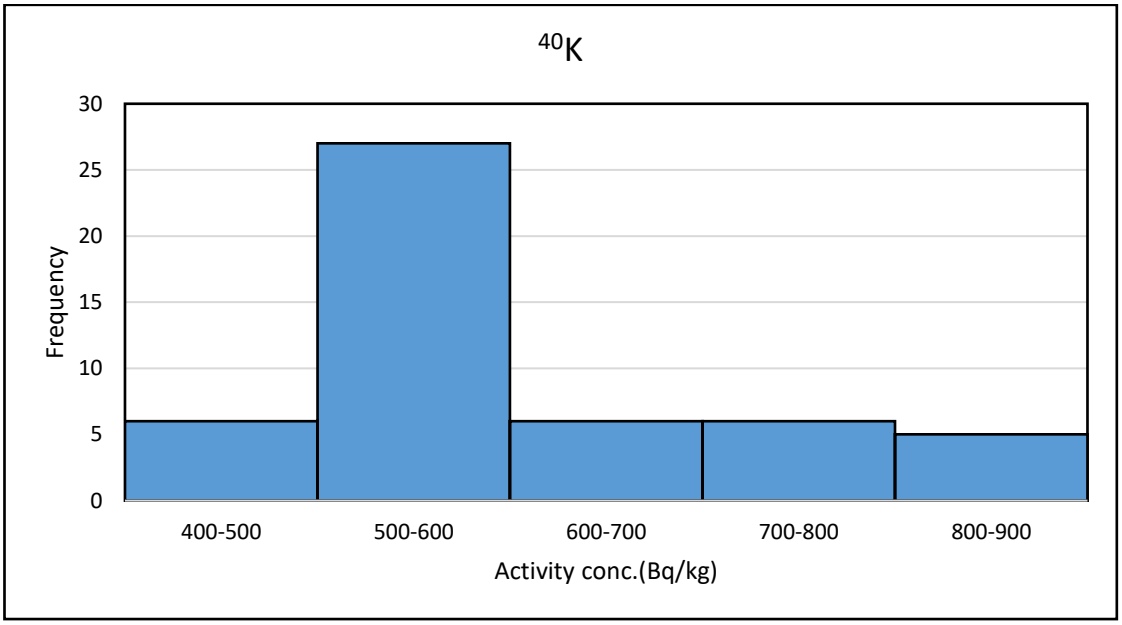

Figure 4.4: Frequency distributions of activity concentrations of ^{40}K in the soil samples

The frequency distribution in Figure 4.2, shows that about 40 samples have activity concentrations of ^{238}U which are above the world-wide mean value of 33 Bq/kg, while a few of the samples (10) have the activity concentrations in the range of 20-35 Bq/kg. Moreover, about 30 samples have ^{238}U activity concentrations of more than 40 Bq/kg. This shows that the activity concentration of ^{238}U is high in most of the samples.

With respect to the frequency distribution of the activity concentrations of ^{232}Th, Figure 4.3 shows that all 50 samples have high activity concentrations which are above the world-wide mean value of 45 Bq/kg, with most of the samples (35) in the activity range of 50-150 Bq/kg.

Similarly, the frequency distributions of the activity concentrations of ^{40}K in all samples are above the world-wide mean value of 420 Bq/kg, with most of the samples (27) in the activity range of 500-600 Bq/kg as shown in Figure 4.4.

Therefore, based on the analysis of the frequency distributions of the activity concentrations of the three radionuclides (^{238}U,^{232}Th & ^{40}K) in all the soil samples, it could be concluded that the distribution is not uninform, and the activity concentrations are high in most of the soil samples.

4.3. Statistical correlations of activity concentrations in Otjiwarongo

Statistical correlation describes the relationship between two related variables e.g. activity concentrations of different radionuclides. When these two variables move in the same direction, their relationship is positive, while when they move in opposite directions, their relationship is negative. The coefficient of correlation (R) which is within the range of -1 to 1 is a measure of correlation relationship between variables.

A correlation of R = -1 is a perfect negative correlation, while a correlation of R = 1 is a perfect positive correlation.

The statistical correlation between activity concentrations of the three radionuclides in the samples are presented from Figure 4.5 to Figure 4.7.

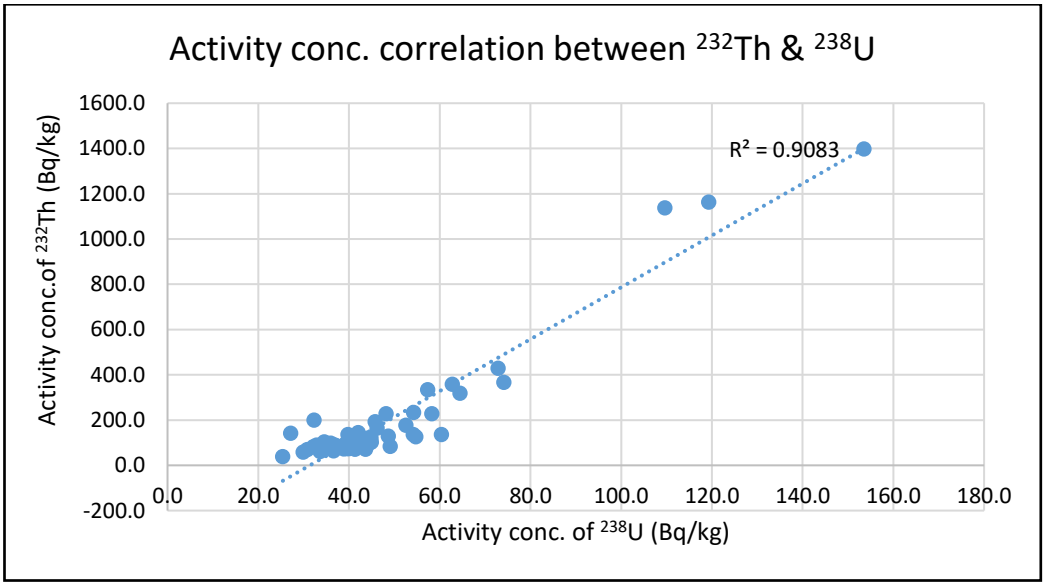

Figure 4.5: Correlation of activity concentrations of ^{232}Th & ^{238}U

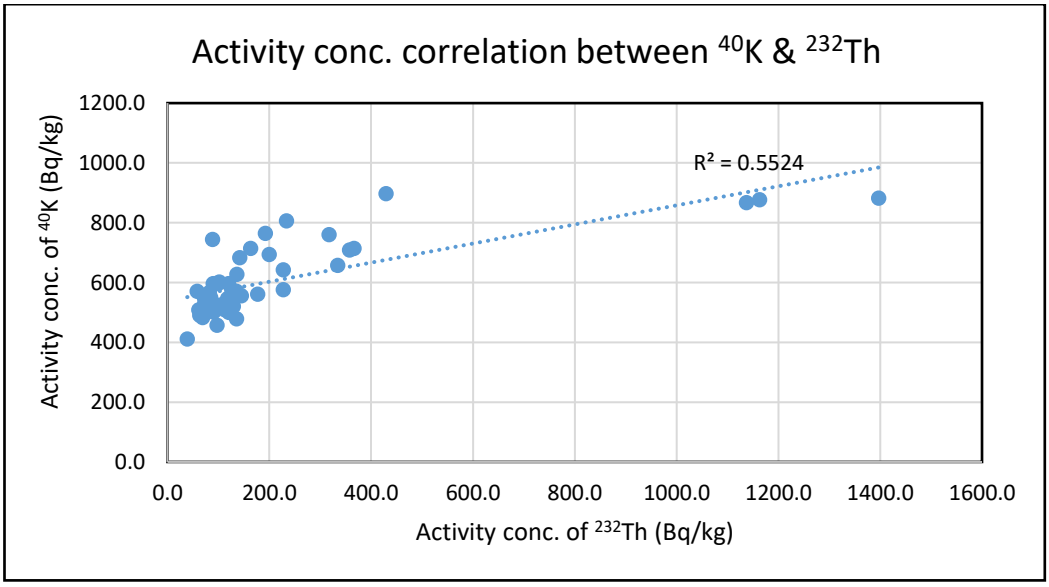

Figure 4.6: Correlation of activity concentrations of ^{40}K & ^{232}Th

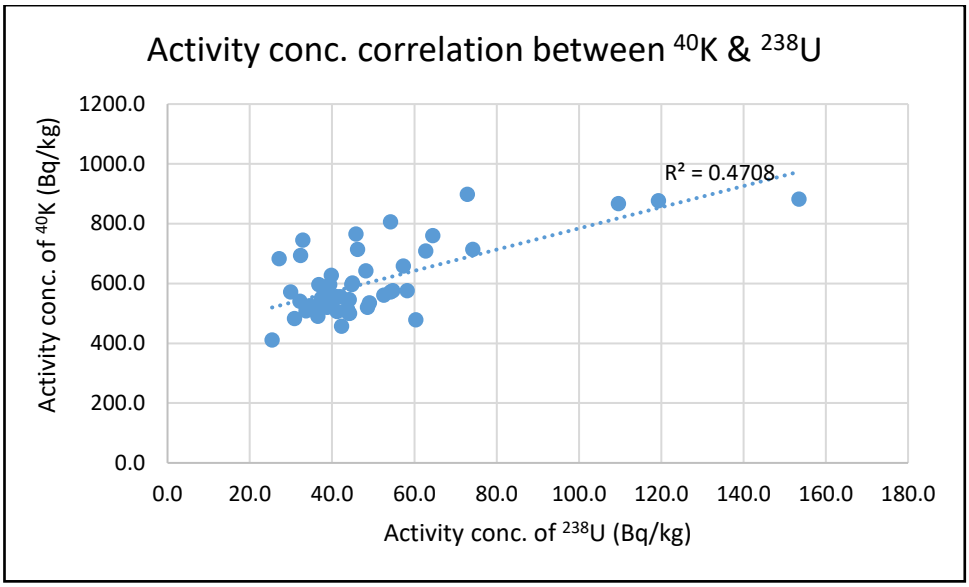

Figure 4.7: Correlation of activity concentrations of ^{40}K & ^{238}U

Figure 4.5 shows that there is a strong positive correlation of 0.9 between the activity concentration of ^{232}Th and that of ^{238}U in the samples. Moreover, a moderate positive correlation of 0.6 is observed between the activity concentration of ^{40}K and that of ^{232}Th, as shown in Figure 4.6, while the activity concentration of ^{40}K and that of ^{238}U has a positive correlation of 0.5 as shown in Figure 4.7. These results show that the correlation between the activity concentrations of different pairs of the three radionuclides in the soil samples is positive.

4.4. Comparison of the mean activity concentrations of ^{238}U, ^{232}Th and ^{40}K in the soils of Otjiwarongo with those measured in the soils of selected towns in Namibia

The mean activity concentrations of ^{238}U, ^{232}Th and ^{40}K in the soils of the town of Otjiwarongo are compared with those of other towns in Namibia, as shown in Table 4.3 and Figure 4.8, [17] .

Table 4.3: Comparison of the activity concentrations of ^{238}U, ^{232}Th, and ^{40}K in different towns in Namibia

Town	Mean concentrations (Bq/kg)		
	^{238}U	^{232}Th	^{40}K
Okahandja	40.9 ± 8.6	57.9 ± 19.4	562.4 ± 125.4
Karibib	29.4 ± 5.8	49 ± 8.6	824.3 ± 153.5
Arandis	72.4 ± 13.5	245.7 ± 87.4	899.7 ± 65.8
Usakos	44.2 ± 9.7	74.8 ± 30.2	959.5 ± 194.7
Swakopmund	46.4 ± 14.2	91.1 ± 39.6	645.5 ± 69.5
Walvis Bay	18.6 ± 4.6	23.8 ± 8.4	460.3 ± 76.2
Wlotzkasbaken	69.6 ±26.3	79.5 ± 44.1	759.2 ± 68.4
Henties Bay	62.2 ± 20.0	97.1 ± 44.7	936.1 ± 68.5
Otjiwarongo	**49.3 ± 23.1**	**204.9 ± 278.2**	**604.3 ± 119.5**

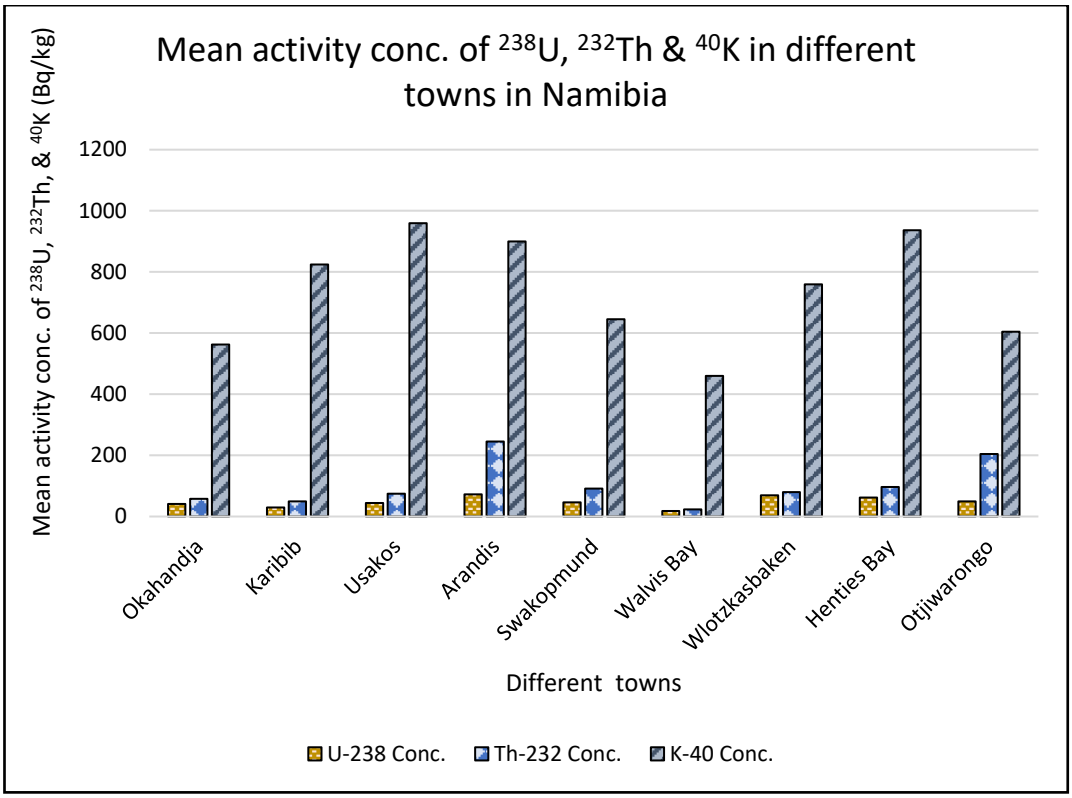

Figure 4.8: Comparison of mean activity concentrations of ^{238}U, ^{232}Th and ^{40}K in different towns in Namibia

The mean activity concentrations of the three radionuclides calculated from Otjiwarongo town was compared to with the mean activity concentrations in other eight (8) towns in Namibia - i.e Okahadja, Karibib, Usakos, Arandis, Swakopmund, Walvis Bay, Wlotzkasbaken and Hentis Bay [3, 11, 26]. A significant difference in the mean activity concentrations of these towns could be clearly seen as shown in Figure 4.8. For instance, the mean activity concentration of ^{232}Th in Otjiwarongo (204.9 ± 278.2 Bq/kg) is much higher than the mean activity concentrations of ^{232}Th in most of the other eight selected towns, (most of which are below 100 Bq/kg) except that of Arandis town. Similarly, the mean activity concentrations of ^{238}U in Otjiwarongo (49.3 ± 23.1 Bq/kg) is slightly higher than most of the eight towns as could be observed in Table 4.3. However, most of the eight towns have high mean activity concentrations

of ^{40}K compared to that of Otjiwarongo (604.3 ± 119.5 Bq/kg). Hence, it could be concluded that the radioactivity level in Otjiwarongo is slightly higher than those of the other eight towns discussed.

4.5. Mean absorbed dose rate and annual effective dose in different areas

The mean absorbed dose rate in air and the mean annual effective dose calculated for each area are shown in Table 4.4.

Table 4.4: Mean absorbed dose rate and annual effective dose in different geographical areas of Otiwarongo (The range of values are given in parenthesis)

Area	Mean absorbed dose rate (nGy /h)	Mean annual effective dose (mSv)
PP	**104.7 ± 19.9** (84.9 - 129.7)	**0.13 ± 0.02*** (0.11 - 0.16)
MP	**91.3 ± 31.9** (52.2 - 130.0)	**0.11 ± 0.04** (0.06 - 0.16)
ME	**99.9 ± 22.2** (76.0 - 130.8)	**0.12 ± 0.03** (0.09 - 0.16)
NW	**94.7 ± 19.4** (83.1 - 126.9)	**0.12 ± 0.02** (0.10 - 0.16)
TL	**100.8 ± 19.6** (72.9 - 117.9)	**0.12 ± 0.02** (0.09 - 0.14)
AP	**133.0 ± 39.4** (97.0 - 188.3)	**0.16 ± 0.05** (0.12 - 0.23)
HA	**90.0 ± 13.7** (73.8 - 100.6)	**0.11 ± 0.02** (0.09 - 0.12)
OT	**184.4 ± 74.3** (99.7 - 255.9)	**0.23 ± 0.09** (0.12 - 0.31)
OR	**593.9 ± 347.2** (164.7 - 951.5)	**0.73 ± 0.43** (0.20 - 1.17)
DR	**225.4 ± 77.1** (149.8 - 330.2)	**0.28 ± 0.09** (0.18 - 0.40)
Mean	**171.7 ± 180.1**	**0.21 ± 0.22**

***annual effective doses given in two decimal places to avoid zero errors**

The mean absorbed dose rate varies from a low value of 90.0 ± 13.7 nGy h^{-1}, at HA area to a high value of 593.9 ± 347.2 nGy h^{-1} at OR area. This shows that the highest mean absorbed dose rate 593.9 ± 347.2 nGy h^{-1} is more than nine times the world average of 60 nGy h^{-1} [2].

The results further show that the mean annual effective dose varies from a low value of 0.1 ± 0.0 mSv at HA area, to a high value of 0.7 ± 0.4 mSv at OR area again.

This implies that the mean effective dose rates calculated for all geographical areas are below the maximum permissible limit of 1 mSv/y recommended by the International Commission on Radiological Protection (ICRP) [27]. Hence, all the effective dose rates obtained are considered to be within acceptable level. These results are shown graphically in Figure 4.9 and Figure 4.10.

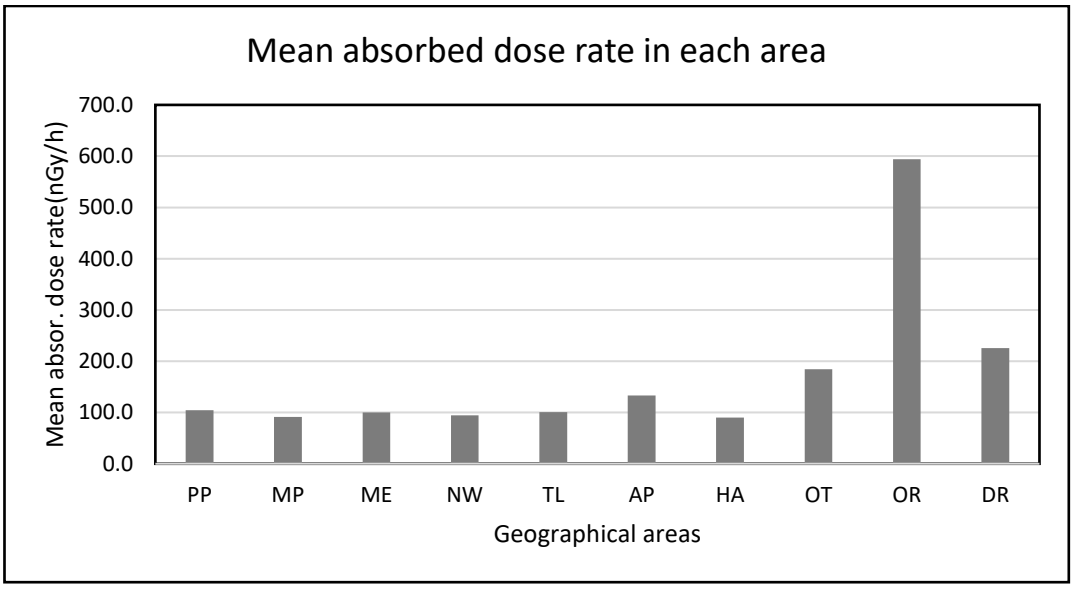

Figure 4.9: The mean absorbed dose rates in different geographical areas of Otjiwarongo

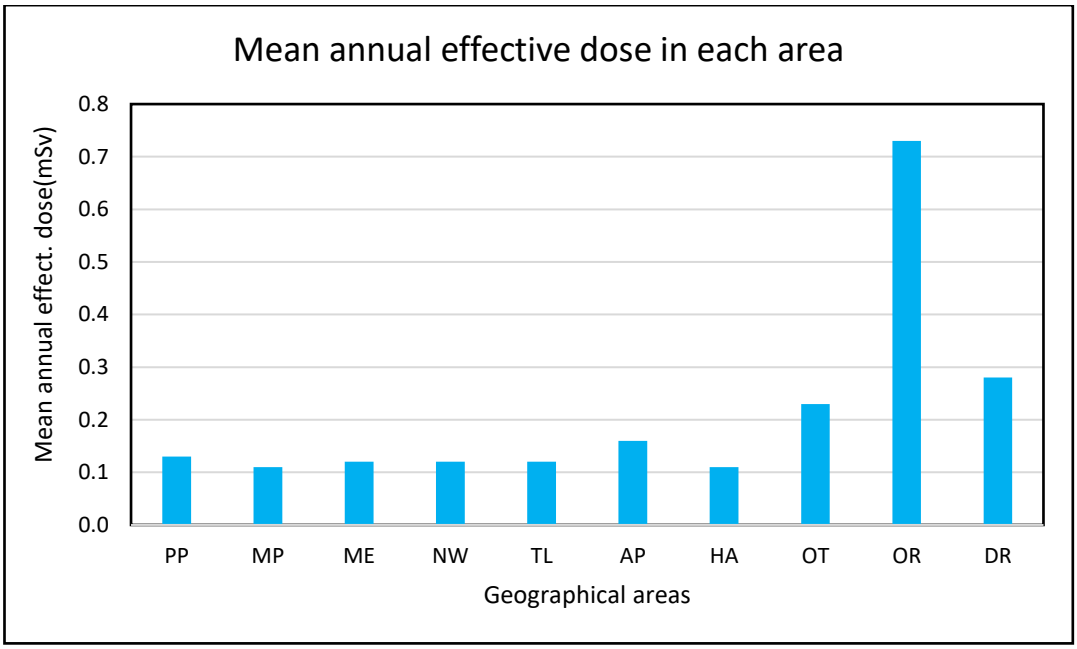

Figure 4.10: The annual effective doses in different geographical areas of Otjiwarongo

4.6. Statistical analysis of the absorbed dose rates and annual effective doses in Otjiwarongo

The descriptive statistics of the results obtained in the measurement of absorbed dose rates and annual effective doses are presented in Table 4.5.

Table 4.5: Statistics of the results obtained in the measurement of absorbed dose rates and annual effective doses in Otjiwarongo

Descriptive statistics	Mean absorbed dose rate ($nGy.h^{-1}$)	Mean annual effective dose (mSv)
Mean	171.7	0.2
Strd. Dev.	180.1	0.2
Median	111.7	0.1
Skewness	3.3	3.3
Kurtosis	10.6	10.6
Min	52.2	0.1
Max	951.5	1.2
Range	899.3	1.1

As could be seen in the Table 4.5, the mean absorbed dose rate is 171.7 $nGy.h^{-1}$ which is much higher than the world-wide mean value of 51 nGy h^{-1} [2]. The data values of absorbed dose rates are widely spread as shown by a large standard error of 180.1 nGy h^{-1}. The distribution of the absorbed dose rates in the town has a kurtosis of 10.6, while with a positive skewness of 3.3.

Also, the mean annual effective dose of the town is 0.2 mSv which is below the ICRP permissible limit of 1mSv. Moreover, the annual effective doses distributions have also a large standard error of 0.21 mSv, with kurtosis of 10.6 due to the spread of the data values. In summary, both the mean absorbed dose rate and the mean annual effective dose of Otjiwarongo have the same skewness and kurtosis values of 3.3 and 10.6 respectively.

The frequency distributions of absorbed dose rates and annual effective doses due to all samples are presented graphically in Figure 4.11 and Figure 4.12 respectively.

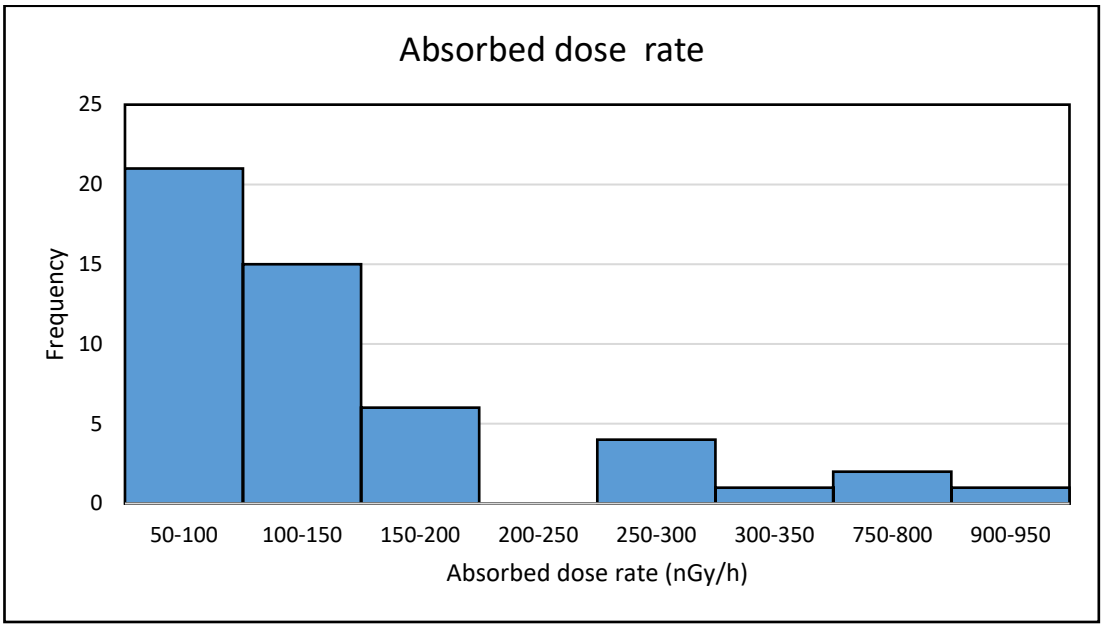

Figure 4.11: Frequency distributions of absorbed dose rates in Otjiwarongo

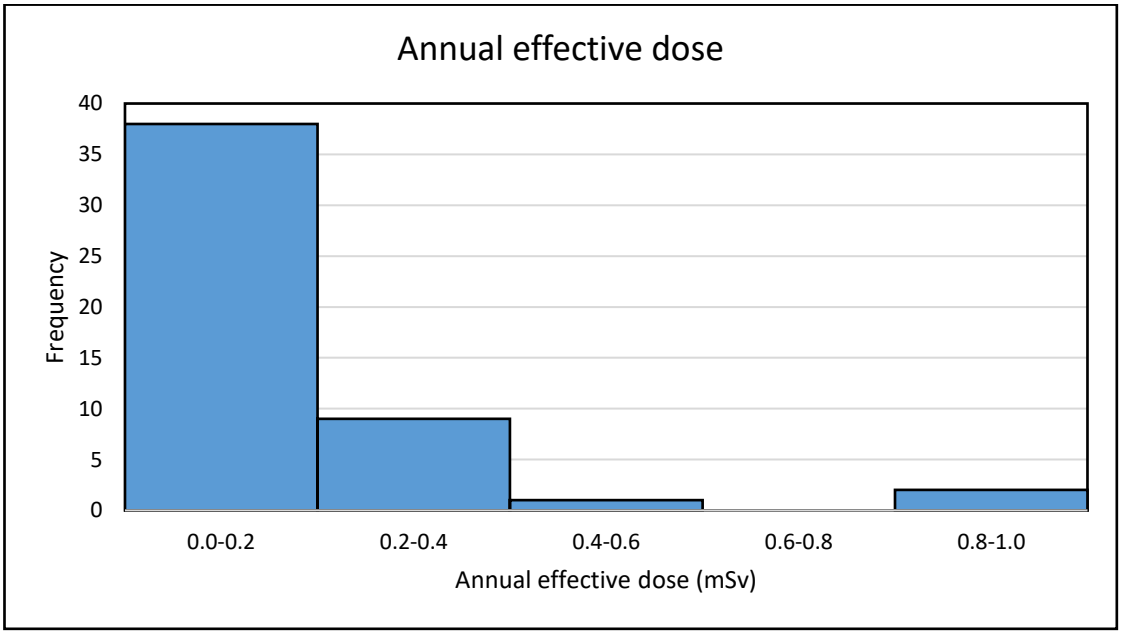

Figure 4.12: Frequency distributions of annual effective doses in Otjiwarongo

It could be observed in Figure 4.11 that 21 samples have absorbed dose rates in the range of 50-100 nGy h^{-1}, while 15 samples have absorbed dose rates in the range of 100-150 nGy h^{-1}. This shows that more than 25 samples have high absorbed dose rates which are above the world-wide mean value of 60 nGy h^{-1}.

For the annual effective dose, the frequency distribution in the histogram 4.12 shows that all the samples fall in the annual effective dose range of 0.00 -1.00 mSv, which is below the ICRP recommended maximum permissible annual limit of 1mSv. This shows that the background radiation is at a normal level in the town.

4.7. Hazard indices in different areas of Otjiwarongo

The mean Radium equivalent activity (Ra_{eq}), external hazard index (H_{ex}) and internal hazard index (H_{in}) in different geographical areas are shown in Table 4.6.

Table 4.6: Mean Radium equivalent activity, external hazard index, and internal hazard index in different areas of Otjiwarongo. (The range of values are given in parenthesis)

Area	Mean Radium equivalent activity (Ra_{eq})	Mean external hazard index (H_{ex})	Mean internal hazard index(H_{in})
PP	**231.6 ± 46.0** (185.0 - 291.1)	**0.6 ± 0.1** (0.5 - 0.8)	**0.8 ± 0.1** (0.6-1.0)
MP	**201.8 ± 73.7** (112.3 - 291.8)	**0.6 ± 0.2** (0.3 - 0.8)	**0.7 ± 0.2** (0.4 – 0.9)
ME	**221.5 ± 50.8** (166.5 - 292.3)	**0.6 ± 0.1** (0.5 - 0.8)	**0.7 ± 0.2** (0.5 – 0.9)
NW	**208.4 ± 44.8** (181.7 - 283.1)	**0.6 ± 0.1** (0.5 - 0.8)	**0.7 ±0.1** (0.6 – 0.9)
TL	**222.4 ± 45.6** (157.3 - 262.0)	0**.6 ± 0.1** (0.4 - 0.7)	**0.7 ± 0.1** (0.5 -0.8)
AP	**298.5 ± 91.6** (215.0 - 427.9)	**0.8 ± 0.3** (0.6 - 1.2)	**0.9 ± 0.3** (0.7 -1.3)
HA	**197.9 ± 31.5** (160.4 - 223.5)	**0.5 ± 0.1** (0.4 - 0.6)	**0.7 ± 0.1** (0.5 – 0.7)
OT	**417.2 ± 173.2** (216.9 - 586.1)	**1.13 ± 0.47** (0.6 - 1.6)	**1.3 ± 0.5** (0.7 – 1.7)
OR	**1379.5 ± 815.7** (371.8 - 2219.1)	**3.7 ± 2.2** (1.0 - 6.0)	**4.0 ± 2.3** (1.1 – 6.4)
DR	**511.0 ± 179.8** (334.8 - 755.5)	**1.4 ± 0.5** (0.9 - 2.0)	**1.5 ± 0.5** (1.0 – 2.2)
Mean	**388.9 ± 426.7**	**1.1 ± 1.2**	**1.2 ± 1.2**

The Radium equivalent activity (Ra_{eq}) ranges from a low value of 197.9 ± 31.5 Bq/kg at HA area to a high value of 1379.5 ± 815.7 Bq/kg at OR area. Similarly, the external radiation hazard index (H_{ex}) ranges from a low value of 0.5 ± 0.1 at HA area to a high value of 3.7 ± 2.2 at OR area. The internal radiation hazard index (H_{in}) ranges from a low value of 0.7 ± 0.1 at both NW, TL and HA areas (column 3) to a high value of 4.0 ± 2.3 at OR area.

These results show that, OR area has the highest Radium equivalent activity (Ra_{eq}), external (H_{ex}) and internal radiation hazard index (H_{in}) while the HA area has the lowest Ra_{eq}, H_{ex} and H_{in} as could be seen in Figure 4.13 and Figure 4.14.

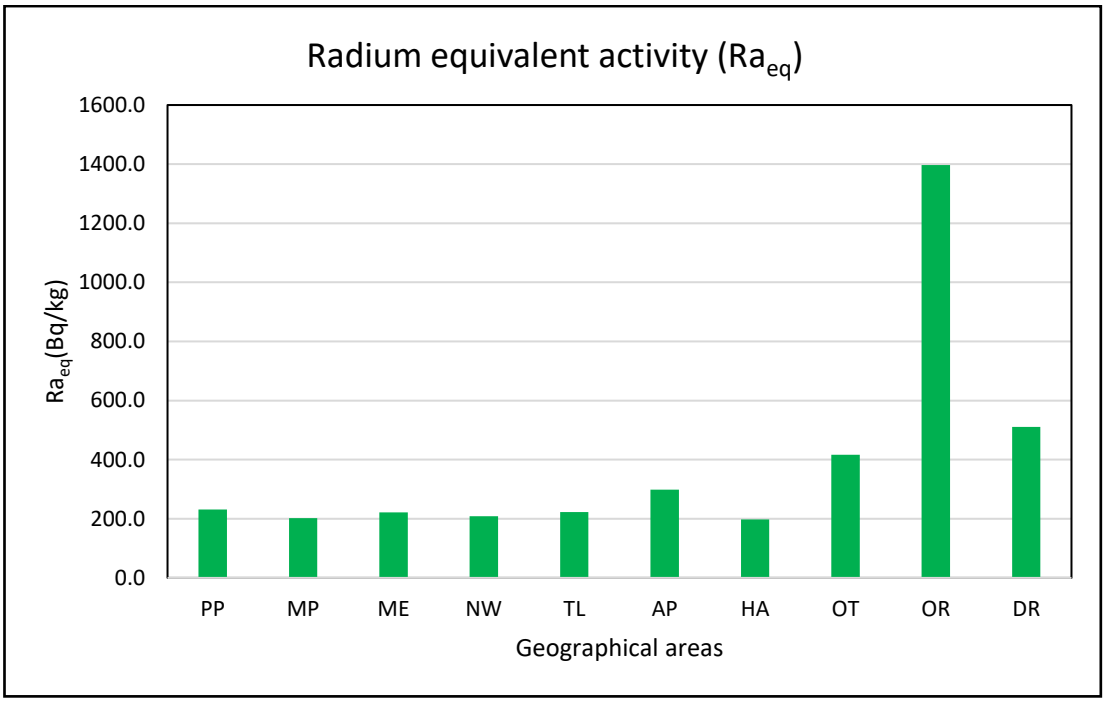

Figure 4.13: Radium equivalent activity in Otjiwarongo

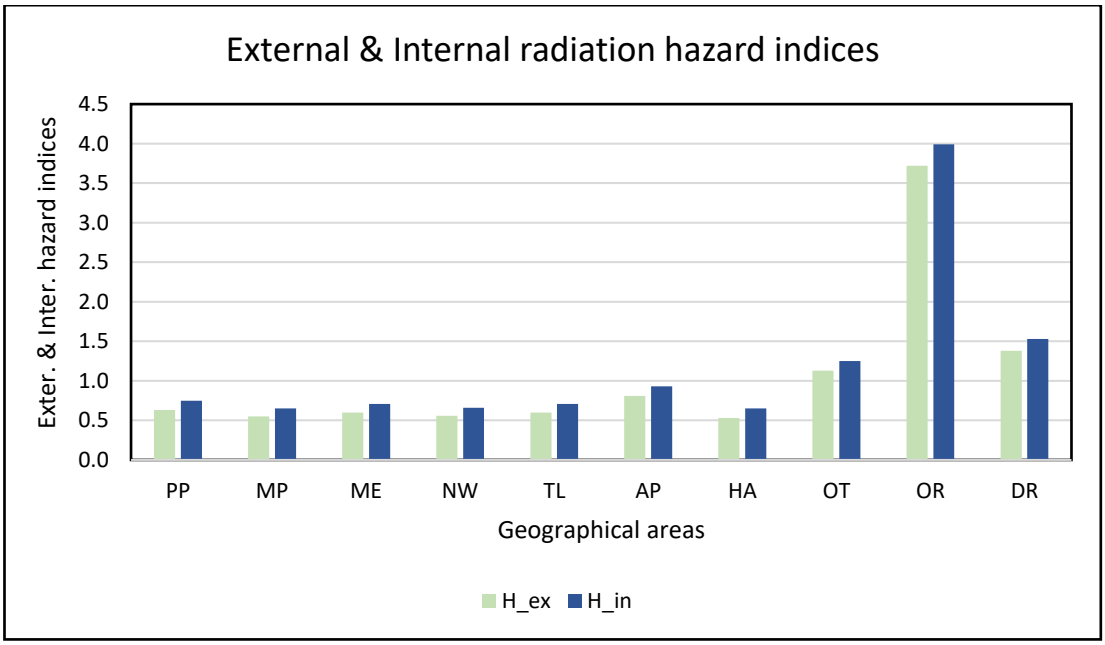

Figure 4.14: External & internal hazard indices in Otjiwarongo

4.8. Statistical analysis of Radium equivalent activity, external, and internal hazard indices in different areas of Otjiwarongo

The descriptive statistics of the Radium equivalent activity, external, and internal hazard indices in different areas of Otjiwarongo are presented in Table 4.7.

Table 4.7: Statistics of the results obtained in the measurement of Radium equivalent activity, external, and internal hazard indices in Otjiwarongo

Descriptive statistics	Radium equivalent activity (Bq/kg)	External hazard index (H_{ex})	Internal hazard index (H_{in})
Mean	388.9	1.1	1.2
Standard Dev.	426.7	1.2	1.2
Median	249.5	0.7	0.8
Skewness	3.3	3.3	3.3
Kurtosis	10.6	10.6	10.6
Min	112.3	0.3	0.4
Max	2219.1	6.0	6.4
Range	2106.8	5.7	6.0

The statistics of the results obtained show that the mean Radium equivalent activity (Ra_{eq}) is 388.9 Bq/kg, which is above the maximum permissible limit of 370 Bq/kg. The distribution of Ra_{eq} in the town has a large standard error of 426.7 which is due to outliers in the distribution. Also, the distribution of Ra_{eq} has a positive Skewness of 3.3 and a Kurtosis of 10.6.

Moreover, the external (H_{ex}) and internal (H_{in}) hazard indices have mean values of 1.1 and 1.2 respectively, which are slightly higher than the maximum permissible

limit of unity. Additionally, both H_{ex} and H_{in} have equal skewness and kurtosis of 3.3 and 10.6 respectively as indicated in Table 4.7.

The frequency distributions of Radium equivalent activity, external and internal hazard indices in Otjiwarongo are shown in Figure 4.15, 4.16, and 4.17 respectively.

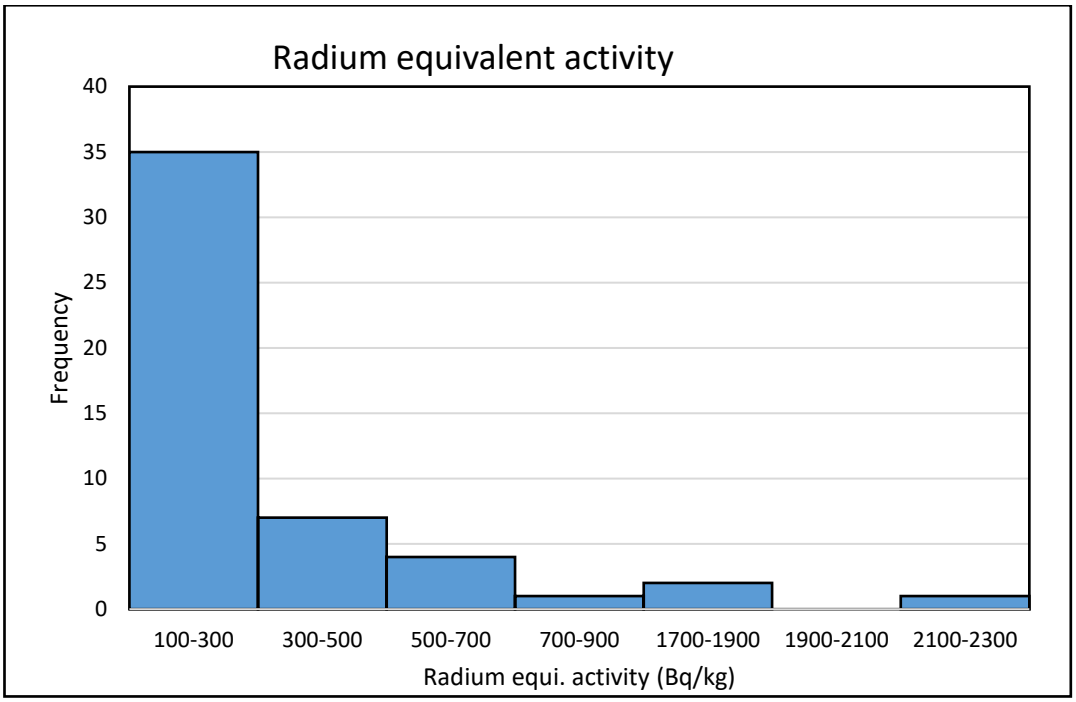

Figure 4.15: Frequency distributions of Radium equivalent activity in Otjiwarongo

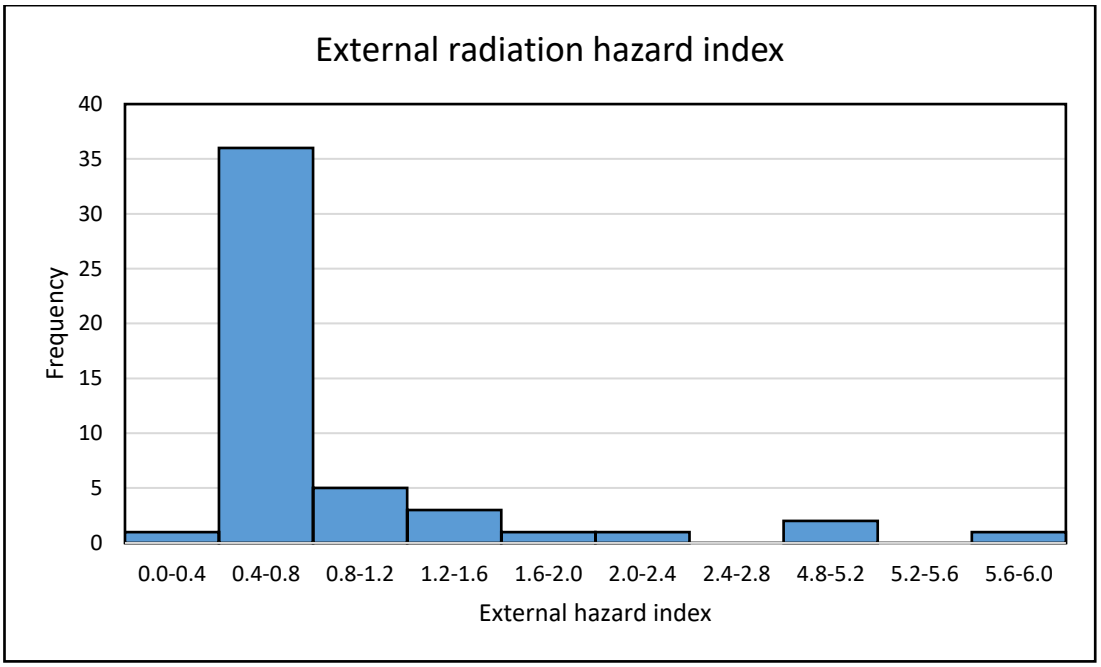

Figure 4.16: Frequency distributions of external hazard index in Otjiwarongo

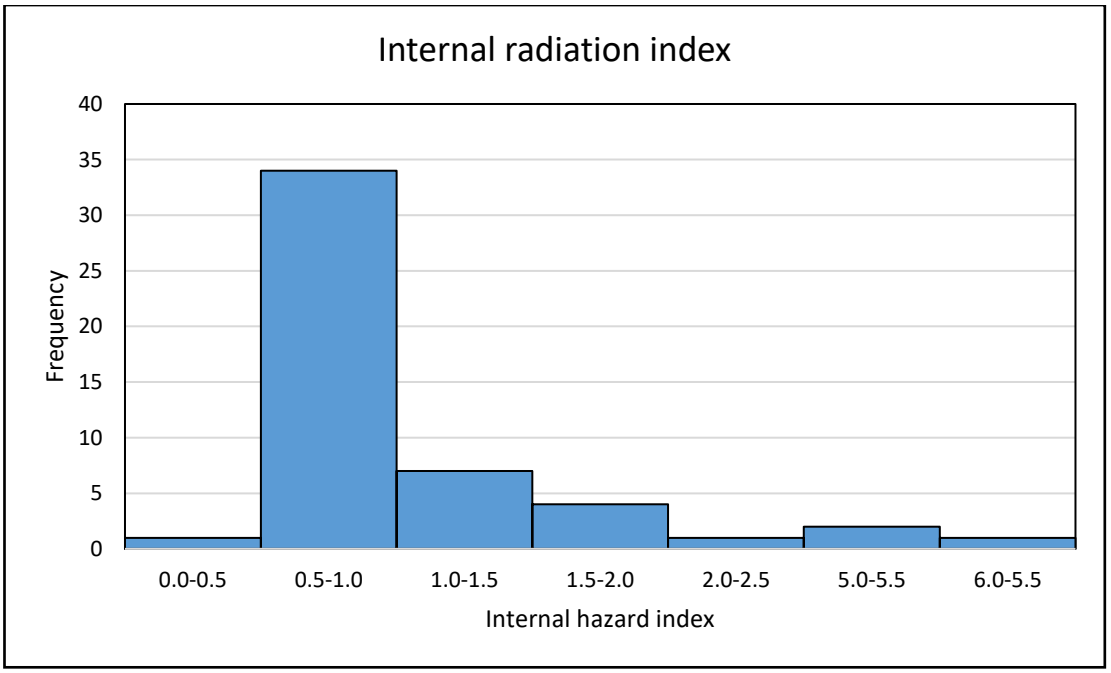

Figure 4.17: Frequency distributions of internal hazard index in Otjiwarongo

As could be observed in Figure 4.15, more than 35 samples have radium equivalent activity (R_{aq}) below the maximum permissible limit of 370 Bq/kg, while more than 10 samples have Raq above the maximum permissible limit. The frequency distribution of the external hazard index in Figure 4.16 shows that more than 35 samples have hazard index in the range 0.40 - 0.80, which is below the maximum permissible limit of unity. Similarly, for the internal hazard index (Figure 4.17) about 35 samples have indices in the range 0.0 - 1.0 which is below the maximum permissible limit of unity. The other 15 samples have hazard indices above the maximum permissible limit of unity. These results confirm that the level of radiation varies across the town of Otjiwarongo but it is well-below the maximum permissible limit in most areas of the town while it is above the maximum permissible limit in some other areas.

CHAPTER 5

5. Conclusion and Recommendations

5.1. Conclusion

The activity concentrations of the three radionuclides ^{238}U, ^{232}Th and ^{40}K, in the soil of the town of Otjiwarongo have been determined using Gamma Spectroscopy. These values were used to calculate the mean activity concentrations of the radionuclides in ten different geographical areas of the town. The mean activity concentrations vary from a low value of 37.6 ± 7.4 to a high value of 97.8 ± 46.2 Bq/kg for ^{238}U; from a value of 81.9 ± 16.7 to a very high value of 852.8 ± 533.0 Bq/kg for ^{232}Th; and from a low value of 498.7 ± 55.7 to high value of 807.1 ± 94.5 Bq/kg for ^{40}K. All these mean activity concentrations are higher than the corresponding world-wide average values. In fact, the mean activity concentrations of some of the radionuclides in some areas are more than double those of the other areas.

The activity concentrations were also used to calculate the radiological parameters associated with the radionuclides in the ten geographical areas. The mean absorbed dose rates in the ten areas are all higher than the world average value of 51.0 nGy h^{-1}. In contrast, the mean effective dose rates are all below the ICRP maximum permissible limit of 1 mSv/y. The mean values obtained for $Ra_{eq,}$ $H_{ex,}$ and H_{in} in some areas are below the corresponding maximum permissible limits but they are above the permissible limits in some areas. These results show that the level of radiation varies across the town of Otjiwarongo. However, the level of radiation in most areas is low while it is high in a few areas.

5.2. Recommendations and Suggestions

The following recommendations and suggestions are made;

- Extensive safety assessments should be carried out in geographical areas of Otjiwarongo having high activity concentrations of the radionuclides (OR, DR and OT areas), in order to determine the exact source of high exposure radiation to the inhabitants and advice the town council accordingly.
- This study should be extended to other major towns in Namibia to determine radiation exposure level of the public.
- Further study may be necessary to estimate internal doses and external doses from other sources like Radon-222 gas from dwellings in Otjiwarongo.
- Lastly, there is a need to improve and strengthen research capabilities of the Nuclear Laboratory for the department of Physics (UNAM). This should include acquisition of a modern gamma spectrometer, which would be efficient and cost-effective, as the current gamma spec is old and not cost-effective in terms of the usage of consumables like Liquid Nitrogen. Also the Nuclear Laboratory has no nuclear technicians to support research-works in the lab, including setting up experiments and assist with equipment operations, malfunctioning and the general up-keep of the lab. It is therefore recommended that a nuclear technician be recruited for the lab.

6. References

[1] F. Khan, "The Physics of Radiation Therapy," *Open Journal of Radiology,* vol. 37, pp. 1374-1375, 2010.

[2] United Nations Scientific Committee on the Effects of Atomic Radiation (UNSCEAR), "Sources and effects of ionizing radiation-Exposures from natuaral radiation sources (annex b)," United Nations, New York, 2000.

[3] S. Shimboyo and J. Oyedele, "Determination of natural radioactivity in soils of Henties Bay, Namibia," *International Science and Technology Journal of Namibia (ISTJN),* vol. 5, pp. 104-110, 2015.

[4] N. Ahmed and A. EL-Arabi, "Natural radioactivity in farm soil and phosphate fertilizer and its enviromental implications in Qena governorate Upper Egypt," *Journal of Enviromental Radioactivity,* vol. 84, pp. 51-64, 2005.

[5] J. Gbadago, A. Faanu, E. Darko and C. Schandorf, "Investigation of the enviromental impacts of naturally occuring radionuclides in the processing of sulfide ores for gold using gamma spectrometry," *Journal of Radiological Protection,* vol. 31, pp. 337-352, 2011.

[6] (UNSCEAR), "Sources and effects of ionizing radiation," United Nations, 1993.

[7] R. Firestone, S. Chu, C. Baglin and J. Zipkin, Table of Isotopes, John Wiley and Sons, 1996.

[8] P. Hodgson, E. Gadioli and E, Introductory Nuclear Physics, UK: UK Oxford University Press, 1997.

[9] W. Burcham and M. Jobes, Nuclear and Particle Physics, United Kingdom: Longman Scientific and Technical, 1995.

[10] R. Tykva and J. Sabol, Low level enviromental radioactivity sources and evaluation, Pennsylvania: Technology Publishing Company, 1995.

[11] S. Shimboyo, J. Oyedele and S. Sitoka, “Soil radioactivity levels and associated hazards in selected towns in Uranium-rich western Namibia,” *International Science and Technology Journal of Namibia,* vol. 7, pp. 73-84, 2016.

[12] J. Konya and N. Nagy, Nuclear and Radiochemistry, Debrecen: Elsevier Inc., 2018.

[13] [Online]. Available: http://formulas.mathcaptain.com/physics/compton-shift-formula.html. [Accessed June 2019].

[14] [Online]. Available: https://www.scienceabc.com/pure-sciences/what-explain-photoelectric-effect-einstein-definition-exmaple-applications-threshold-frequency.html. [Accessed June 2019].

[15] G. Knoll, Radiation Detection and Measurement, New York: John Wiley & Sons, 2010.

[16] [Online]. Available: http://hyperphysics.phy-astr.gsu.edu/hbase/Relativ/releng.html. [Accessed June 2019].

[17] S. Shimboyo, “Natural Radioactivity in soil of the Walvis Bay and Henties Bay Coastal area,” University of Namibia, Windhoek, 2013.

[18] [Online]. Available: https://en.wikipedia.org/wiki/Geiger-Muller_tube. [Accessed June 2019].

[19] [Online]. Available: https://www.s-cool.co.uk/assets/learn_its/alevel/physics/radioactivity/cloud-and-bubble-chambers/a-phy-radrad-dia0b.gif.

[20] [Online]. Available: https://www.s-cool.co.uk/assets/learn_its/alevel/physics/radioactivity/cloud-and-bubble-chambers/a-phy-radrad-dia0cc.gif. [Accessed June 2019].

[21] E. Taapopi, “Assessment of naturally occuring radioactive materials and trace elements in playgrounds of selected basic schools in thec GA east municipal district, Accra, Ghana,” University of Ghana,, Lego, Accra, Ghana, 2015.

[22] A. Faan, E. Darko and J. Ephraim, “Determination of natural radioactivity and hazard in soil and rock samples in a mining area in Ghana,” *West African Journal of applied ecology ,* vol. 19, no. 1, 2012.

[23] WNA, “Nuclear Radiation and Health Effects,” London, UK, 2018.

[24] J. Oyedele, S. Sitoka and I. Davids, “Radionuclide concentrations in soils of northern Namibia and Southern Namibia,” *Radiation Protection Dosimetry,* vol. 131, 2008.

[25] H. Beck, J. DeCompo and J. Gologak, “In-situ Ge (Li) and NaI(TI) gamma-ray spectrometry, Report 258,” U.S Atomic Energy Commission, 1972.

[26] W. Midzi, “Measurement of natural radioactivity and dose rate assessment of terrestrial gamma radiation in the soils of Karibib and Okahandja, Namibia,” *International Science and Technology Journal of Namibia,* vol. 13, pp. 60-74, 2019.

[27] ICRP, “1990 Recommentations of the International Commission on Radiological Protection,” Oxford, UK, Pergamon Press, UK, 1991.

7. Appendices

Python analyses codes

```
Python 3.3.3 (v3.3.3:c3896275c0f6, Nov 18 2013, 21:18:40) [MSC
v.1600 32 bit (Intel)] on win32

Type "copyright", "credits" or "license()" for more information.
# program calculates the concentration (Bq/kg) of the nuclides U-
238,Th-232,K-40 in a given sample with net peak area U for U-238, Th
for Th-232 and K for K-40

# it also calculates the Dose rate in nGy/h and the Effective dose
rate in mSv/y

Import math
import numpy as np
f = open ('netpeakareas.txt','r')  #opens the file and reads the
results for U, Th and K Net peak Areas and their errors
contents = f.readlines() # list the contents of the opened file as
strings

# The following code creates an empty list to input net peak areas
of U, U1, Th, Th1, K and K1 in samples
U =[]
U1 =[]
Th =[]
Th1 =[]

K =[]

K1 =[]

for lines in contents:
   spl = lines.strip().split()      #split the lines into columns
   if len(spl)==6:                  # split lines into 6 columns
      a,b,c, d, e, j = lines.split()  # assigns each column to a, b,
c, d, e, f

#The following code appends columns a,b,c,d,e,j into empty lists for
U,Th,K,U1,Th1 and K1
      U.append(float(a))
      Th.append(float(c))
      U1.append(float(b))
```

```
        Th1.append(float(d))
        K.append(float(e))
        K1.append(float(j))
```

 # The following code creates an array of net peak areas U, Th, K and an array of errors on net peak area U1,Th1 and k1

```
U = np.array(U)
U1 = np.array(U1)
Th = np.array(Th)

Th1 = np.array(Th1)

K = np.array(K)

K1 = np.array(K1)
```

#the following codes assigns the values of the net peak areas, concentrations and their errors for U-238, Th-232 and K-40 in the standards

#it also calculates k for U-238,Th-232 and K-40 in the standards

```
A_Us = 73200.00

Ae_Us = 302.59

C_Us = 4939.99

Ce_Us = 29.99

k_U = A_Us/C_Us

ke_Us = ((((Ae_Us/A_Us)**2+(Ce_Us/ C_Us)**2)*(k_U)**2)**0.5)

A_Ths = 21400.00

Ae_Ths = 148.75

C_Ths = 3249.99

Ce_Ths = 89.99

k_Th = A_Ths/C_Ths

ke_Ths = ((((Ae_Ths/A_Ths)**2+(Ce_Ths/ C_Ths)**2)*(k_Th)**2)**0.5)

A_Ks = 27500.00

Ae_Ks = 165.81

C_Ks = 14000.00
```

```
Ce_Ks = 400.00

k_K = A_Ks/C_Ks

ke_Ks = ((((Ae_Ks/A_Ks)**2+(Ce_Ks/ C_Ks) **2)*(k_K)**2)**0.5)

For n in U, U1, Th, Th1, K, K1: # this loop calculates the
concentrations and the errors on the concentrations of the
radionuclides in the samples

      U_c = U/k_U

      U_ce = ((((U1/U_c)**2+(ke_Us/k-U)**2)*(U

      -c)**2)***0.5)

      Th_c = Th/k_Th

      Th_ce = ((((Th1/Th_c)**2+(ke_Ths/k-Th)**2)*(Th

      -c)**2)**0.5)

      K_c = K/k_K

      K_ce = ((((K1/U_c)**2+(ke_Ks/k-K)**2)*(K

      -c)**2)***0.5)

for p in U_c, Th_c, K_c, U_ce, Th_ce, K_ce:#calculates the absorbed
dose and their errors

      Dt = 0.042* K_c + 0.429*U_c + 0.666*Th_c

      Dt_er = ((((0.042*K_ce)**2 + (0.429*U_ce)**2 +
(0.666*Th_ce)**2))**0.5)

for q in Dt, Dt_er:  #calculates the effective dose and the errors
on the effective dose

      A_eff_Dose = Dt*0.00876*0.7*0.2

      A_eff_Dose_er = Dt_er*0.00876*0.7*0.2

z = open ('results.txt','w')

z.write ('U_c \t U-ce \t Th_c \t Th_ce \t \t K_c \t \t \t K_ce \t
Dse_rt \t Dse_rt_er \t A_ef_dse \t A_ef_dse_er \n')

i = 0
```

```
for i in range (0,50):

  z.write ('%2.2f \t %2.2f \t \t %2.2f \t \t %2.2f\t \t %2.3f \t \t
%2.2f \t \t %2.2f \t \t %2.2f \t \t %2.3f \t \t %2.3f \n'%(U_c[i],
U_ce[i],Th_c[i],Th_ce[i],   K_c[i],   K_ce[i],   Dt[i],   Dt_er[i],
A_eff_Dose[i], A_eff_Dose_er[i]))

i += 1

f.close()
```

Isotope activity concentrations of ^{238}U, ^{232}Th and ^{40}K in the soils of Otjiwarongo

	Isotope concentrations in Otjiwarongo (Bq/kg)					
Sample	**^{238}U**	**Error in the conc. of ^{238}U**	**^{232}Th**	**Error in Conc. of ^{232}Th**	**^{40}K**	**Error in conc. of ^{40}K**
DR-1	46.18	2.35	163.36	7.50	714.29	27.50
DR-2	54.24	2.79	233.59	9.29	806.12	29.96
DR-3	72.87	3.65	429.01	14.46	897.96	32.89
DR-4	62.75	3.63	357.25	12.47	709.18	27.86
DR-5	45.79	2.74	192.37	7.76	765.31	28.93
NW-1	38.11	2.40	82.14	4.49	566.33	23.36
NW-2	32.18	1.98	81.83	4.82	540.82	22.42
NW-3	39.98	2.28	72.82	4.70	556.12	22.88
NW-4	38.82	2.30	71.91	4.49	520.41	21.84
NW-5	39.79	2.55	136.34	6.54	627.55	25.14
ME-1	38.76	2.08	76.03	4.81	530.61	22.32
ME-2	42.31	2.54	97.10	5.26	457.65	19.98
ME-3	30.83	2.20	68.85	4.57	483.16	20.82
ME-4	54.17	2.76	135.73	6.46	571.43	23.75
ME-5	43.85	2.23	112.67	6.08	508.67	21.50
MP-1	44.24	2.24	120.31	5.92	500.00	21.78
MP-2	42.05	2.59	144.73	6.92	556.12	23.20
MP-3	25.41	1.76	38.63	3.54	411.22	18.66
MP-4	39.53	2.31	73.44	4.76	535.71	22.43
MP-5	36.57	2.30	63.05	4.32	490.31	21.22
PP-1	36.76	2.18	89.92	5.50	596.94	24.21
PP-2	60.36	2.88	135.57	6.40	478.57	21.16
PP-3	54.75	2.71	125.95	6.58	576.53	23.97
PP-4	41.34	2.34	70.53	5.00	556.12	22.91
PP-5	41.21	2.44	77.56	4.66	507.14	21.59
OR-1	109.63	5.58	1137.40	34.14	867.35	33.57
OR-2	32.31	2.77	200.00	7.99	693.88	26.85
OR-3	119.31	5.86	1163.36	34.80	877.55	34.05
OR-4	74.16	3.85	366.41	12.84	714.29	28.05
OR-5	153.49	5.97	1396.95	41.20	882.65	35.60
OT-1	32.89	2.26	88.55	5.30	744.90	27.98
OT-2	57.33	2.29	334.35	11.84	658.16	26.56
OT-3	27.15	2.48	141.98	6.71	683.67	26.36
OT-4	64.49	3.00	317.56	11.34	760.20	28.89
OT-5	48.17	2.90	227.48	8.79	642.86	25.87
AP-1	35.99	2.24	97.40	5.29	515.31	21.96

AP-2	48.63	2.75	129.01	6.22	520.41	21.97
AP-3	58.24	2.85	227.48	9.17	576.53	23.93
AP-4	52.56	2.81	177.10	7.69	561.22	23.53
AP-5	39.40	2.18	99.39	5.56	596.94	24.08
HA-1	34.57	2.16	103.82	5.63	525.51	21.99
HA-2	44.05	2.48	90.23	5.80	501.02	21.89
HA-3	43.66	2.34	70.53	4.60	515.31	21.49
HA-4	49.08	2.56	83.51	5.07	535.71	22.62
HA-5	33.66	2.05	61.22	4.12	509.18	21.52
TL-1	37.40	2.28	84.89	4.98	551.02	22.74
TL-2	29.92	2.02	58.32	4.13	571.43	23.04
TL-3	44.18	2.67	118.02	5.96	545.92	22.90
TL-4	44.82	2.53	119.69	6.17	596.94	24.00
TL-5	44.95	2.46	101.68	5.41	602.04	24.19

Mean radioactivity concentrations in different geographical areas

	Mean Activity Concentration (Bq/kg)					
Area	**^{238}U**	**Error in mean conc. of ^{238}U**	**^{232}Th**	**Error in mean conc. of ^{232}Th**	**^{40}K**	**Error in mean conc. of ^{40}K**
DR	56.37	11.55	275.11	113.46	794.64	77.68
NW	37.78	3.22	89.01	26.89	562.24	40.40
ME	41.98	8.47	98.08	27.25	510.31	43.76
MP	37.56	7.37	88.03	43.40	498.67	55.66
PP	46.88	10:11	99.91	29.21	543.06	49.1
OR	97.78	46.24	852.82	532.98	807.14	94.52
OT	46.01	15.83	221.99	107.23	697.96	52.21
AP	46.96	9.20	146.08	55.74	554.08	35.46
HA	41	6.65	81.86	16.65	517.35	13.61
TL	40.26	6.58	96.52	25.59	573.47	25.66